We thank the reviewers for their helpful comments. The comments and suggestions have been addressed accordingly. Thank you for your time and effort. The replies to each comment are shown in blue.

Reviewer 1:

In this study, Bryant et al. examined the formation of isoprene-derived SOA (iSOA) during summer in Beijing (China) using a large suite of online and offline instruments. In particular, the authors focus on LC-MS data from filter extracts of PM2.5 and the detection, identification, and quantification of isoprene-derived organosulfates (OSs) and nitrooxy-organosulfates (NOSs). They determined an average concentration of iSOA OSs and NOSs of 82.5 ng m–3. Moreover, the authors claim that OS formation depends on a combination of photochemistry and particulate sulfate concentrations, and suggest that iSOA formation is strongly controlled by anthropogenic emissions in Beijing.

The authors acquired an impressive dataset with state-of-the-art instruments during their field study. Moreover, molecular-level identification and quantification of SOA constituents, such as OSs and NOSs, is challenging, yet highly desirable. However, I see several major weaknesses in the measurement approach, the data analysis and interpretation of the results, which need to be addressed before I can recommend the publication of the manuscript (as detailed below).

Major comments:

1) I have the impression that the main conclusion (which is also the title) of the manuscript is only weakly supported by the data shown in the manuscript. The authors claim that there is a "strong anthropogenic control of SOA formation from isoprene in Beijing". However, only one figure (i.e., Figure 5) is actually showing a weak correlation of OSs to the product of ozone and sulfate concentrations, which can be considered to some extent as a metric for anthropogenic influences. Nonetheless, no correlations of total SOA mass to common anthropogenic pollutants is shown or discussed. It should also be noted that particulate sulfate could have been transported to the sampling site over longer distances, and thus, is not a direct anthropogenic emission factor.

There was a similar comment from all three reviewers and so we have added an additional section on the gas phase data (see reply to comment 2) to show the concentrations and trends of anthropogenic tracers in Beijing. We have also added a PollutionRose plot (new Figure 2) of particulate sulfate concentrations, which shows a strong anthropogenic source of particulate sulfate to the south of Beijing which contains a large industrial region. While the sulfate is likely formed outside the city, it is still an anthropogenic tracer. We also discussed in the paper the effect of NO (an anthropogenic tracer) on the products formed and have added additional clarification of the role of biogenic-anthropogenic interactions in the formation mechanisms of the products. Finally, we have shown the moderate to strong relationship with the product of sulfate and ozone, which are both secondary pollutants formed from anthropogenic emissions. We have moved Figure S10 into the main manuscript (new Figure 5) which shows the degree of correlation for all isoprene OS SOA tracers against each other and with a range of anthropogenic tracers.

We have added the following text to address this comment:

"The isoprene SOA tracers identified in this study are correlated towards themselves as well as common anthropogenic tracers in a corplot (Openair, R), shown in Figure 5. The corplot highlights the correlations of the iSOA tracers to each other as well as the moderate to strong correlations towards some of the anthropogenic pollutants as discussed in further sections."

"As such, this tracer is the result of a direct biogenic-anthropogenic interaction."

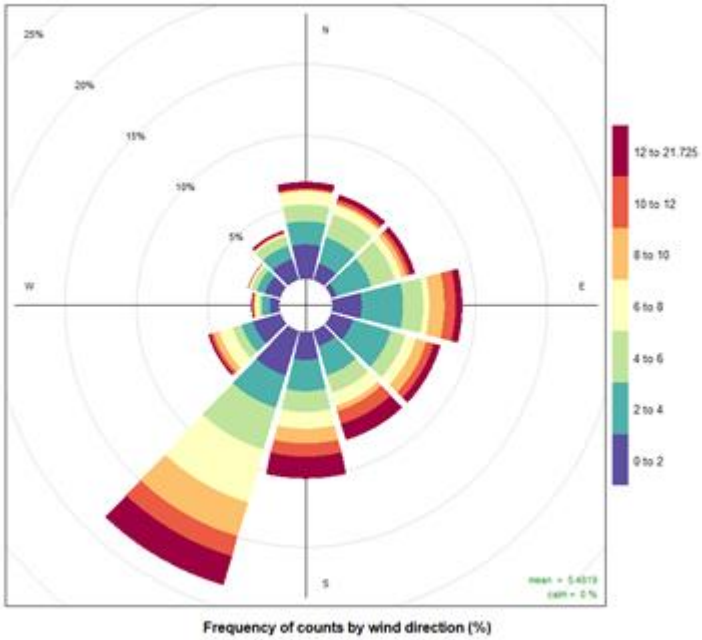

"**Figure 2.** PollutionRose plot (Openair) of particle sulfate measured by AMS, during the sampling period."

2) In general, the discussion of the data remains quite superficial in several sections, which might also be one of the reasons for my comment above. For example, Fig. 1, which displays typical anthropogenic pollutants, is barely discussed in the results section (i.e. only four sentences, P8L315–318). This is similar for several other figures in the manuscript. Moreover, the authors should reconsider the order and layout of the figures, as the reader is often forced to jump between figures or to find essential data in the SI (e.g., Fig. S10).

There have been a number of publications concerning the gas phase data presented and so we did not want to repeat that discussion in length here. However, in response to reviewer 1 and 2, we have added a small section discussing the concentrations and trends of the data in Figure 1. We have also moved figure S10 to the main paper in response to the reviewers paper.
We have added the following text to address this comment::

"3.2 Anthropogenic tracers

A range of gas phase anthropogenic tracers were measured during the campaign as discussed in Shi et al., 2019. Figure 1 shows the time series of NO, NO_2, O_3 and particulate sulfate during the part of the campaign analysed in this study. Table 1 shows the average, maximum and minimum concentrations for these anthropogenic pollutants. NO mixing ratios ranged from less than 0.1 ppbv to 104 ppbv, and a mean concentration during the filter sampling period of 5.1 ppb. The highest concentrations generally occurred in the morning 04:00-07:00 and steadily decreased during the day. On some days, the mixing ratio of NO was very low in the afternoon, as a result of reaction with ozone and other unknown sinks (Newland et al., 2020). The mean mixing ratio of NO_2 was 22.3 ppbV, much higher than NO, with a range of 3.7 to 95 ppbv. NO_2 peaked between 06:00-07:00 and decreased to a minima at 14:00 and then steady increased until about 20:00. High afternoon concentrations of O_3 (>80 ppb) were found on most days, with a maximum observed mixing ratio of 182 ppbv. Night time O_3 levels were much lower due

to reduced photochemistry and reaction with NO, although on some nights O_3 levels were maintained above 40 ppbv, as shown in Figure 1. Particulate sulfate concentrations, measured by AMS are also shown in figure 1. Sulfate ranged from 0.7 to 21.7 μg m^{-3}, with an average of 5.5 μg m^{-3}. The time series shows a number of periods of high sulfate concentrations and these generally matched periods of increased $PM_{2.5}$ (see Figure 9). Figure 2 shows the wind direction dependent concentrations of particulate sulfate for the sampling period in a pollutionRose plot (Openair package, R). There is a strong source of sulfate from the south of the sampling site, which is enhanced under the highest wind speeds. Previous studies have shown a strong source of pollution from the south west of Beijing, which is where many industrial factories are located (Wang et al., 2005).

3a) One of my most pressing concerns is the LC-MS method used for filter extract analysis and the selection of reversed-phase LC for the separation and detection of isoprene-derived OSs. As can clearly be seen from Table 1, the OSs are not retained on the column and probably elute together with inorganic salts such as sulfate. For example, 15 of the 31 identified species have a retention time of <0.8 min. For these compounds, it is actually impossible to exclude ionization artefacts, i.e., the corresponding compounds are formed from inorganic sulfate and organic compounds during electrospray ionization. It would be necessary to give at least the dead time of the LC system, to make the reader aware of such potential artefacts.

Sulfate and nitrate ions elute in the dead time of the column at 0.67 min. Thus these inorganic ions are offset from the OS species, although there is still some co-elution. We analysed a subset of the filters using normal phase HILIC separation and found a strong correlation between the sum of the 2MT-OS isomers and the single mixed isomer peak found using the reverse phase analysis method (R^2 =0.85). Considering the two methods extract into different solvents (water v methanol) this suggests that there is no significant formation of OS species in the ion source. To test for artefact formation of OS in the sources, we analysed a sample containing a large excess of ammonium sulfate with 2-methyltetrol and 2-methylglyceric acid authentic standards. No 2-MG-OS formation was observed and <0.5% conversion was seen for the 2-MT. The combination of both pieces of evidence, excludes the formation of OS in the source. In addition, if OS species form from reactions between oxidised species and sulfate in the ion source, then all previous direct infusion studies would also suffer from this interference. We have added text to clarify this and included this new test.

Added text:

"Due to the wide range of compounds studied, poor retention was observed for some species (RT < 0.8min). These species closely eluted to the dead time of the column where inorganic sulfate ions eluted (0.67 min). To check for ionisation artefacts, a aqueous solution containing 20 ppm ammonium sulfate, 1ppm 2-methytetrol and 1ppm 2-methylglyceric acid was ran under the same conditions as the filter samples to check for organosulfate formation (2-MT-OS and 2-MG-OS respectively). No MG-OS formation was observed and <0.5% conversion was seen for the 2-MT."

"The sum of peak areas from the 2-MT-OS isomers measured by HILIC and the quantified 2-MT-OS (sum of isomers) measured via UPLC/ESI-HR-MS were compared and showed a high degree of correlation (R^2 = 0.84), even though the two methods used different solvents. The agreement indicates that the UPLC/ESI-HR-MS method captures the sum of the isomers and there is no evidence of ion source induced artefacts."

3b) Moreover, the authors state that potential isoprene OSs were "identified" based on previous studies and then searched for in the LC-MS data (cf. P5L204f). However, even with high mass accuracy and resolving power, it is not possible to identify compounds without any reference standards. I can imagine that there were actually several isomers detectable for each of the "identified" OSs in Table 1 (actually, the authors even admit
the presence of isomeric species in the following section 2.4). How did the authors decide which retention time to take for each of the OSs from the literature?

We thank the reviewer for highlighting our confusing use of the word identified here. For the majority of the OS species in this study, the separation was not good enough to separate isomers and a single peak was observed in the extracted chromatograms for each *m/z*. The MS^2 spectra for each peak was checked for characteristic OS fragmentation patterns. There were only two available authentic standards and so these compounds have been identified in this work (although these still include a number of co-eluting isomers). It is possible that some of the iSOA OS observed here may have other

sources as we highlight in the paper. For the NOS, the individual isomers could be resolved and are presented in the paper. We have replaced the confusing text.
Following text was changed:
"Using previously observed iSOA products from literature, extracted ion chromatograms were plotted for each *m/z* value from a small subset of ambient samples and the retention time (RT) of observed species/isomer were obtained. For most of the OS species in this study the separation was not good enough to see individual isomers and only one peak was observed, which was added to the library. For the NOS species, individual isomers could be resolved, and each isomer was added to the library based on its retention time."
L222 : "Tracefinder extracted the OS/NOS tracer peak areas from each ambient sample chromatogram using the library based on RT and accurate mass."

4) The authors claim that they account for matrix effects by calibrating the LC-MS through a standard addition approach. However, in my opinion, this approach is far from convincing, as only 6 of the 132 filters (i.e., 4.5%) of all filters were actually investigated. Moreover, it seems quite unreasonable to me to take the calibration curve of 2-MG-OS for all other detected OSs. As shown in Fig. S2, the slope of 2-MT-OS is about 4x larger than for 2-MG-OS. Eventually, such differences in sensitivity might lead to a large overestimation of OSs concentrations. This has to be discussed in more detail. Merely stating that the measurement uncertainty is 60% is not sufficient. How did the authors actually calculate this uncertainty?

We disagree with the reviewers comments on using the 2-MG-OS to represent the other iSOA compounds. The 2-MT-OS calibration line using standard addition is only 2.33 times higher than the 2-MG-OS external calibration, compared to around 10 times higher using the 2-MT-OS external calibration. If we used the external calibrations we would have significantly **underestimated** the concentration of the 2-MT-OS species. It is true, that using proxys to calibrate the other iSOA could result in issues during the calibration. However, this careful analysis was carried out to minimise the effects of using just a single external calibration to estimate concentrations. We have added additional text to discuss the potential for underestimating the concentrations without taking matrix effects into account. The 60 % uncertainty was used to account for the difference in the observed correction factors used when correcting for matrix effects.
added text:" this uncertainty was calculated to account for the difference in the measured correction factors used when correcting for the matrix effects."
added text: " Further work is needed to fully understand the reasons. Without these additional standard addition calibrations, the iSOA concentrations would have been largely underestimated."

Specific comments:
1) As one of the main aspects of the manuscript is the quantification of OSs and NOSs, I was wondering if the introduction may benefit from some more information on the general abundance of OSs also from other precursors such as monoterpenes and/or alkanes (e.g., Wang et al. JGR 2017, doi: 10.1002/2017JD026930; Brüggemann Environ. Chem. 2019, doi: 10.1071/EN19089; Riva et al. ACP 2016, doi:10.5194/acp-16-11001-2016)
The following text has been added:
"SOA formed from anthropogenic and other biogenic (monoterpenes and sesquiterpenes) sources have also been studied. Thousands of organic species including hundreds of OS and nitroxy OS (NOS) species have been identified studies from a range of precursors using UPLC/ESI-HR-MS from ambient aerosol samples (Wang et al., 2016, Wang et al., 2017). Brüggemann et al. (2019) quantified with authentic standards both monoterpene OS (MT-OS) and sesquiterpene OS (SQT-OS) species in Melpitz, Germany and Wangdu, China. They found median daytime concentrations for Melpitz and Wangdu for 52 MT-OS species of 12.15 ng m^{-3} and 38.19 ng m^{-3} respectively. For the 5 SQT-OS species, median concentrations were 0.3 ng m^{-3} and 3.90 ng m^{-3} for daytime concentrations respectively, much lower than the iSOA OS species quantified in this study. Riva et al. (2016) identified OS species from the photo-oxidation of C_{10} – C_{12} alkanes, which were then characterised in ambient aerosol samples collected in Lahore, Pakistan and Pasadena, CA, USA. High concentrations of OS species were identified in Lahore, with the largest observed concentration arising from a cycodecane OS species ($C_{10}H_{16}O_7S$) with a concentration of 35.93 ng m^{-3}. "

2) P5L174: As the samples were only extracted using H2O, it is important to state that only the water-soluble fraction of the filter samples was analyzed.

The following text has been added: "The water-soluble fraction of the filter samples were analysed"

3) P5L175: Did the authors account for potential artifacts from sonication of the filter samples, for example, as shown by Mutzel et al. (Atmos. Environ. 2013, doi:10.1016/j.atmosenv.2012.11.012)

Additional experiments comparing sonication and an orbital shaker found no appreciable difference in the concentrations of iSOA tracers analysed in this study.

Following text has been added:

"A small subset (3) of the filter samples were also extracted via orbital shaker and no appreciable difference was found in the concentrations of the iSOA tracers compared to sonication."

4) P5L191: What is "full scan MS2"? Do the authors mean full scan combined with data-dependent fragmentation (i.e., full scan-ddMS2)? If so, how many different ion species were fragmented after each full scan? And how were they selected? Moreover, the authors should state at which resolution the mass spectra were obtained, as this will also determine the chromatographic time resolution of the MS method. Besides,
it also remains unclear if and how many replicate injections were performed for each sample.

The following text has been added:

"analysed using UPLC-full scan-ddMS^2"
", with a resolution of 70,000"
", each filter sample was run only once."
" The number of most abundant precursors for MS^2 fragmentation per scan was set to 10"

5) P6L216: Here, it is necessary to explain what standards were used for the calibration curves. Without this knowledge, it is very confusing for the reader to follow this discussion.

This section is simply discussing how the data was handled, and therefore doesn't go into detail surrounding how the calibrations were achieved. The quantification including standards are discussed in section 3.3. We have added a sentence to direct the reader to the later section.

Following text has been added:
"(as discussed in section 3.3)"

6) Section 2.5: The filter extraction method for the HILIC-MS analysis is very different from the LC-MS method. In this case, pure methanol was used for extraction. Did the authors investigate how this affects the presence of certain OSs and NOSs?

This was not carried out as only a small subset of filters were analysed and thus whether extraction in methanol favours certain species over other has not been determined. However, the 2-MT-OS data obtained using both methods show a strong correlation as mentioned above, but unfortunately the HILIC method was not calibrated at the time.

7) P8L300: It is stated that a SIFT-MS was used to measure isoprene, however, there are no data shown from these measurements. The authors merely claim that there is a good correlation to the DC-GC measurements (P8L321)

The DC-GC Isoprene diurnal profile is shown in figure 3 and the full time series is shown in figure 1. We did not show the sift data since it was taken at a height of 100 m up the tower. We only used the SIFT data to compare the correlation of the iSOA species with both techniques, as they cover slightly different time periods due to instrument maintenance and down-time.

8) Fig. 1: I would recommend avoiding interpolation over periods of missing data.
Again, as mentioned above, there is almost no discussion of the data.

This has been addressed with a new section 3.2. Interpolation across periods of missing data removed.

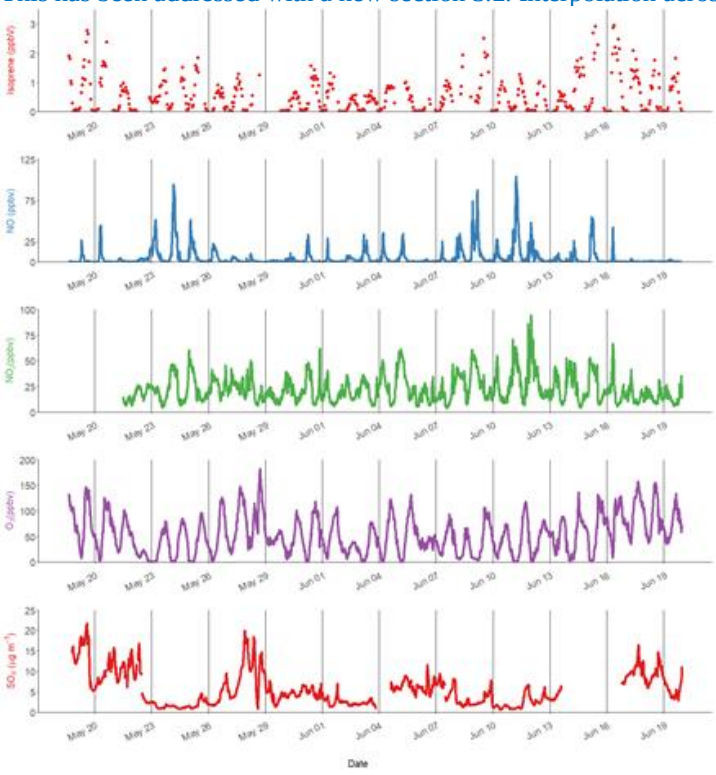

9) P8L328: Give values for k_ox in the main text and not only in the caption of the figure.
Following text has been added:
L343: "The IUPAC rate constants that were used in the calculation for NO_3, O_3 and OH were $7x10^{-13}$, $1.27x10^{17}$, $1x10^{10}$ cm^3 $molecule^{-1}$ s^{-1} respectively."
10) Fig. 3a: I would recommend giving the loss rate in ppb h-1, as this would help the reader to compare the numbers to the actual measurements. Moreover, you could try to estimate a lower limit for isoprene emissions here and compare it to previous studies.

We have added a figure showing the values in ppb hr-1. We cannot estimate the isoprene emission as we don't know the reaction time between emission and measurement and since this is a biogenic emission, photochemical age calculations are unlikely to give useful information.

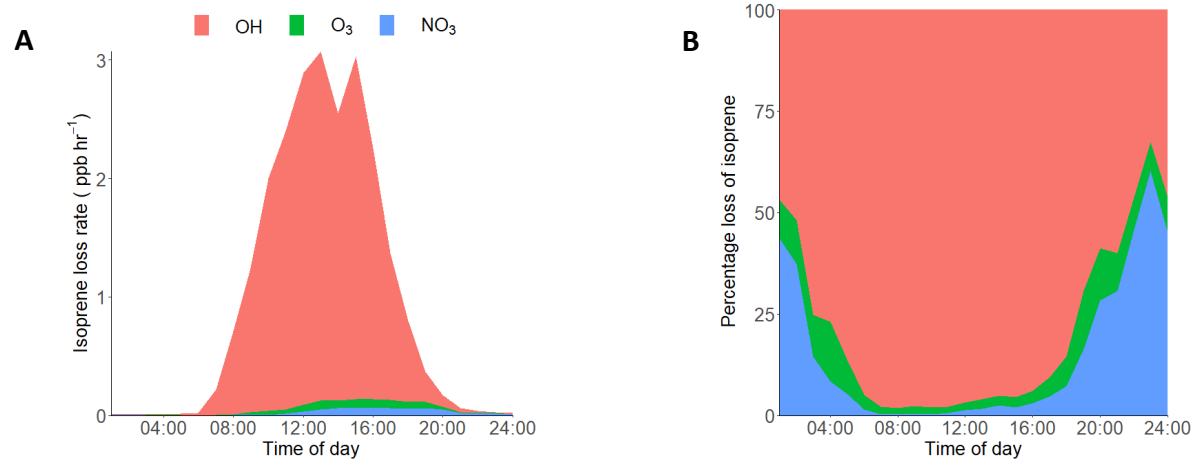

Figure 4. (A) Diurnal loss rate of isoprene calculated using measured average diurnal profiles of isoprene, OH, NO_3 and ozone. (B) Average diurnal of the percentage loss of isoprene from reactions with OH, O_3 and NO_3 radicals.The IUPAC rate constants used for the calculations are as follows, NO_3: $7x10^{-13}$, O_3:$1.27x10^{17}$, OH: $1x10^{10}$ cm^3 $molecule^{-1}$ s^{-1} (Atkinson et al., 2006).

11) P9L349 / Fig. S2-S4: The calibration curves are not of high quality. Especially, for the lower concentrations the data seem to deviate quite strongly from the determined fits (Fig. S2). It would be nice to see errorbars for the variability / standard deviation of the data. Why is the standard addition only shown for one filter sample each? You could normalize the data and show how the slopes of the calibration curves compare to the external calibration for the two compounds.

There is only a small deviation at the lower concentrations, with both calibrations showing a good linear fit. Error bars have been added to the calibration curves. Only one standard addition per filter sample was carried out due to having a limited amount of sample. We did present all of the standard addition sample data (i.e. the comparison of slopes) in the Table S1 and S2 but from the reviewers comment this is not clear to the reader. The additional text we have added in response to comment 12 clarifies this.

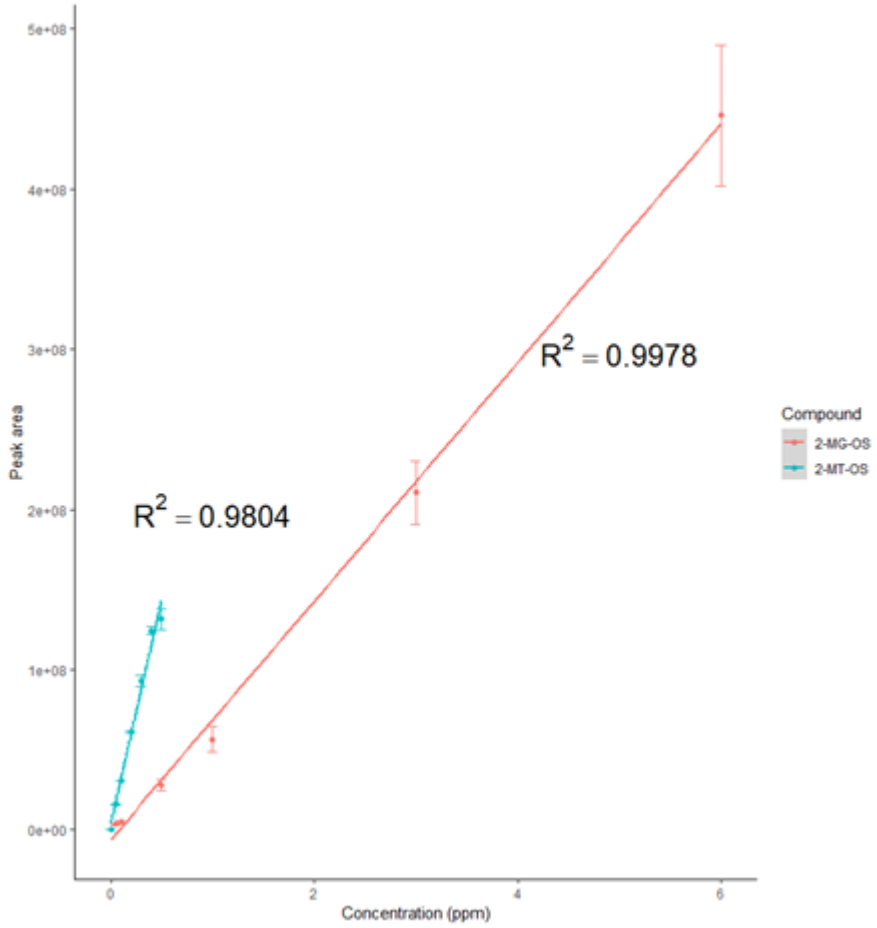

12) P9L354 / Table S1 and S2: How did the authors select these filter samples? There is no further information given on how these filters were selected and whether they are representative for the campaign period. Moreover, Tables S1 and S2 are very difficult to comprehend.

This sentence in the text already describes how these filters were selected:

"Five-point standard addition calibrations were run on 6 different filter extracts, covering both day and nighttime samples, during periods of both high and low concentrations of iSOA species."

An additional paragraph has been added to improve understanding of tables S1 and S2.

"Table S1 shows the concentration of 2-MT-OS in three filter sample extracts (144, 204, 208) calculated via standard addition of 2-MT-OS to the filter sample extract and via external calibrations using both 2-MT-OS and 2-MG-OS. The ratio of the standard addition to the external calibrations then gives an estimate of the under or overestimate the external calibrations make to calculating the concentration of 2-MT-OS in the samples. Both the external calibrations would lead to an underestimation of concentration of 2-MT-OS in the filter samples. 2-MG-OS provided a closer quantification of 2-MT-OS in the samples, with an average factor of 2.3 underestimation, while the 2-MT-OS external calibration gives a sample concentration a factor of 10 lower than the standard addition determined concentration."

13) P10L372: Where do these scaling factors come from?
This has been addressed in response to comment 12.

14) P10L374: How did the authors calculate an uncertainty of 60% for their concentrations? If there is such a high uncertainty, it should clearly be stated also in Table 1.

This is addressed above. We do not feel it is necessary to add this to the table.

15) Fig. 4: It is misleading to represent the concentrations of the quantified compounds by single data points and to interpolate in between. Better display concentration steps with corresponding lengths to the sampling time.

We have modified the figures to show the start and end time of the samples but kept a data point at the mid sample time and the interpolation between points. Using simple bars made the plot very difficult to read, especially as there are over 100 sample points.

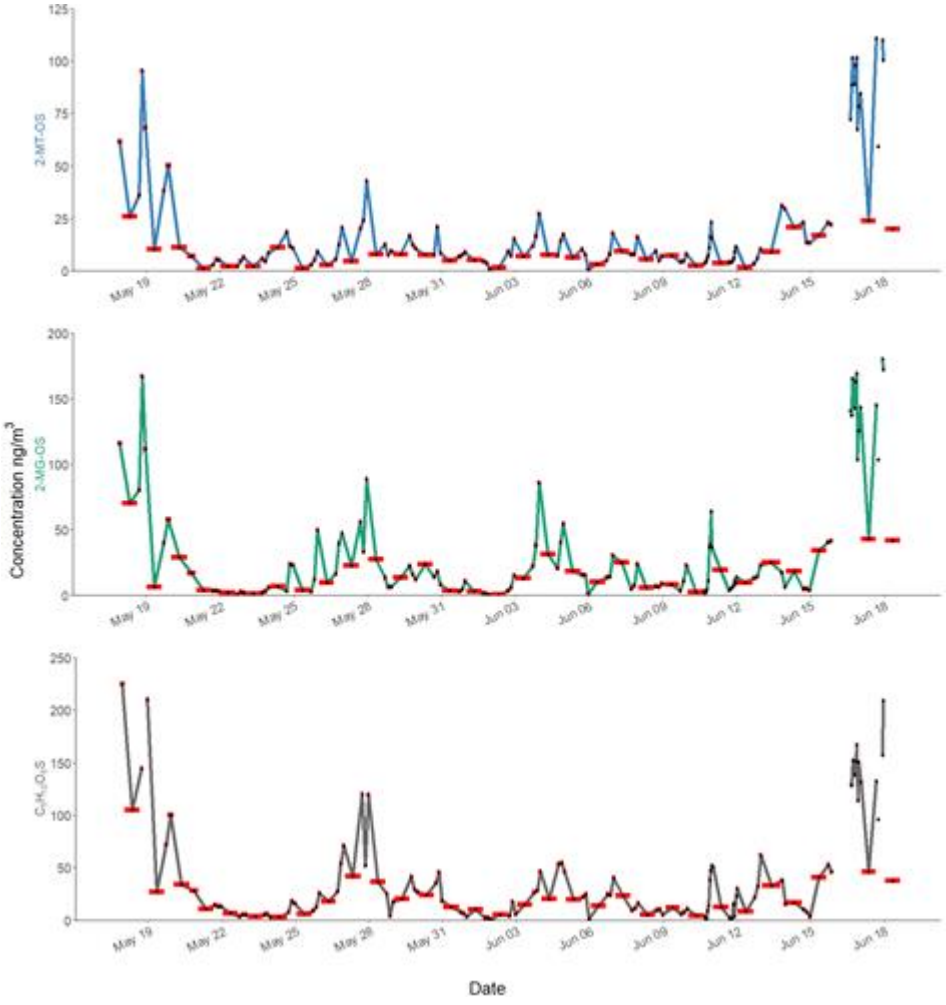

16) P10L394: The reader has to believe the authors that the three-hourly data are consistent with the hourly samples. No evidence is shown for this assertion.

Both figures 2 (now 3) and S10 (now 8) show the diurnal variation of 2-MT-OS and 2-MG-OS respectively during the hourly sampling and shows that the 1 hourly is consistent with the 3 hourly data. The hourly filters were taken during the highest pollution event, and so is expected to show higher concentrations.

17) P10L398–P11L413: It would be helpful for the reader to see all the data discussed in this section in one figure. Furthermore, it would be much more convincing to see correlation plots instead of time series (also in other parts of the manuscript).

A Corplot has now been added to the main manuscript to highlight the correlations between all known iSOA species and anthropogenic pollutants. This clearly shows the high correlation of different types of iSOA with each other, with the daytime peaking OS in the top right and the NOS towards the middle of the plot. The gas phase tracers are in the bottom corner. This plot also includes both [SO42-] and [O3][SO42-] and the higher correlations with the latter can be seen.

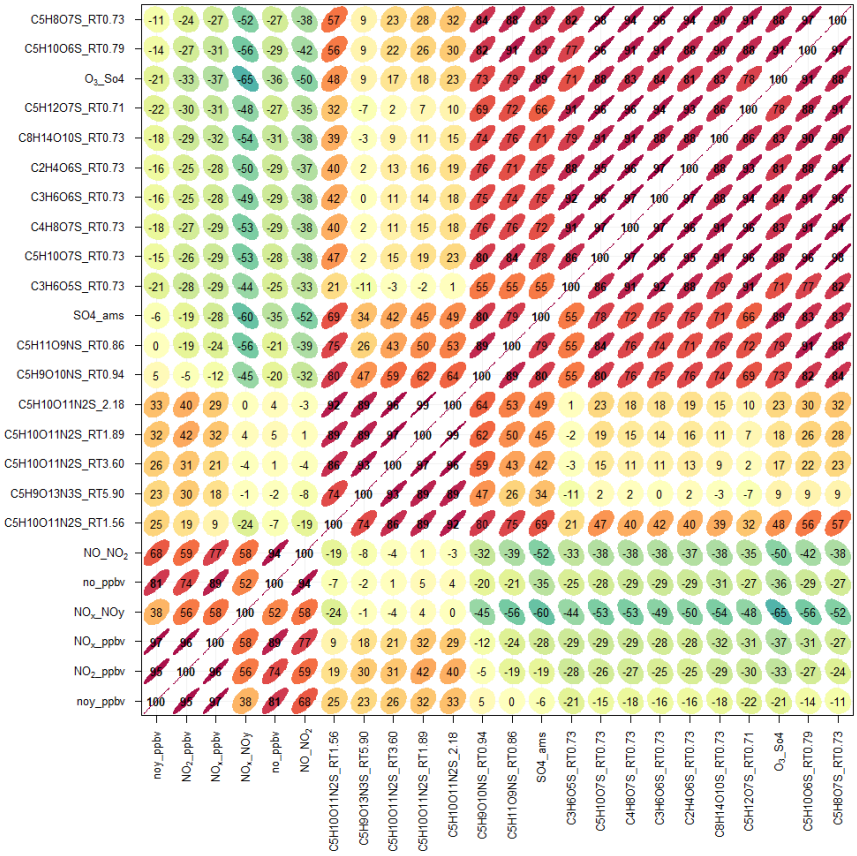

360

Figure 5. Corplot (Openair) highlighting the correlations between known iSOA tracers and anthropogenic pollutants. The number represents the R correlation between the two species. With redder more elongated circles highlighting a higher correlation.

365 18) Fig S7 / P11L416: It is obvious that especially OSs with similar retention times(i.e., 0.71–0.73 min) strongly correlate with each other. This is a strong indication that ionization artifacts produce these species (e.g., fragments, adducts, complexes, etc.),as they are all ionized at the same time in the ESI source. The authors should discuss and clearly state this in the manuscript.
See reply to comment 3a.

370

19) P11L421: Any references which support this hypothesis?
This sort of correlation has not been seen previously as far as we are aware and so no reference can be included.

375 20) Fig. S8: The figure has a bad quality and typos in the title. Moreover, the caption is not sufficient to understand the content of the figure.

We agree that the labels on the plot have gone wrong during the conversion to pdf. This has been rectified. We have added additional text to the caption.

380

New figure caption: "**Figure S7:** Extracted ion chromatograms (m/z 215.0) using hydrophobic interaction liquid chromatography (HILIC) of 2-methyltetrol OS (2-MT-OS) isomers, highlighting improved separation of isomers using this technique. Upper: Extract of filter collected on the 28/05/2017 between 11:33 and 14:23. Lower: 10 ppm 2-MT-OS standard (Cui et al., 2018)."

385

21) P11L445: Do the authors mean regional background sites? (also at P12L450)

This has been addressed.
Text added: “background”

22) Fig. S10 / P12L463: Why is the Figure in the SI? It is an essential part of your data. Any hypothesis why the concentrations are higher at night?
Moved into the main paper. We are not sure what the second part of this comment refers to?

23) Fig. 6: It would be beneficial to see a comparison to total PM or OM mass concentrations in the figure.
We have added PM2.5 into an upper panel on figure 6 for comparison.

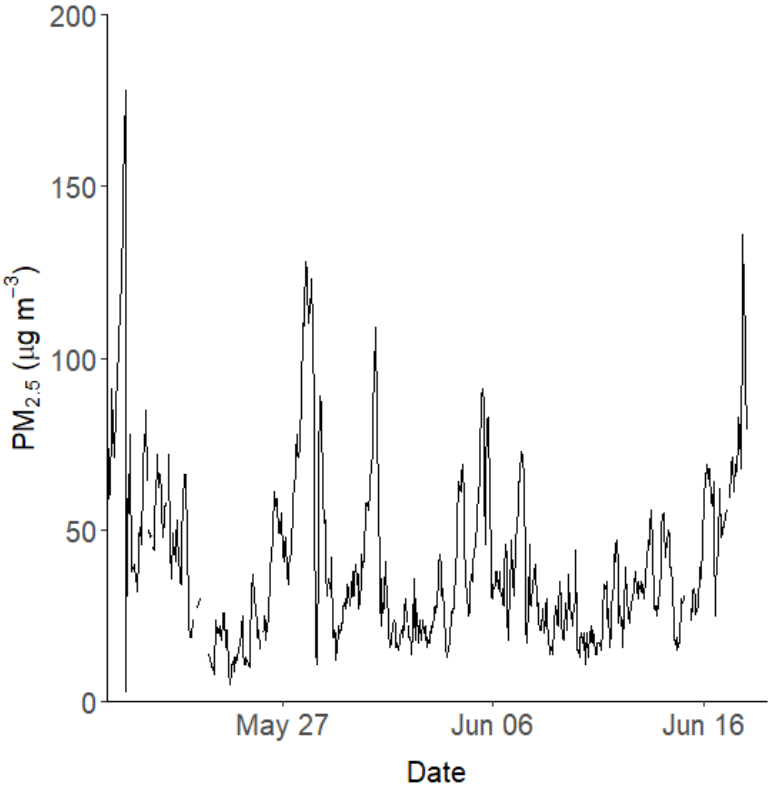

24) P13L526: There are no corresponding data shown to this discussion.
A table (Table 3) has been added to show the min, max and mean concentrations of the CHO species measured via GC-MS. The following has been added:

“Table 3. Isoprene CHO tracer concentrations measured via GC-MS using 24 hour samples between 22/05/2017 and 22/06/2017. 2-MTs is equal to the sum of 2-methylthreitol and 2-methylerythritol and the C5-alkene triols is equal to the sum of cis-2-methyl-1,3,4-trihydroxy-1-butene, 3-methyl-2,3,4-trihydroxy-1-butene and trans-2-methyl-1,3,4-trihydroxy-1-butene.”

Isoprene Tracer	Min (ng m^{-3})	Max (ng m^{-3})	Average (ng m^{-3})
2-MTs	4.55	52.67	17.29
MG	1.38	15.53	7.24
C_5-alkene triols	0.23	1.08	0.51

25) P14L546: So far, there was no clear discussion of NOx levels and how they affect iSOA formation in Beijing.

This has been addressed by the response to comment 2.

Technical comments:

1) P5L184: What is "UPLC-MS2"? I think this term is very misleading here. If I understood the methods section correctly, the authors use full scan data for the quantification of the target analytes.

We do indeed use full scan for the quantification but we also use the MS2 to check that the species fragment to give typical OS fragment ions. This has been added to the text.

Following text was added:

"It should be noted that MS^2 was used to check that the iSOA species fragmented to give typical OS fragment ions."

2) P9L341: The wording "high throughput screening" is quite exaggerated. The method described here is more like a standard data processing method of LC-MS data.

The high throughput represents the analysis time, which at 16 min is shorter than previous methods. By building the library of dedicated iSOA species, we have also significantly reduced the analysis time.

3) P9L355: I do not understand what the sentence "50 _L of filter sample extract and : : :" should tell the reader here.

In the pdf version we downloaded this sentence says 50 MICRO(μ) L

4) P9L367: Use the notation "Table S1 and S2" to avoid confusion

This has now been changed.

5) P10L389: I do not understand what this sentence should tell us here. Is this an important comparison to AMS data?

This information shows that under these conditions the AMS cannot replicate the type of isoprene PMF factors analysis that can be done in more isoprene dominated regions.

6) P14L540: Instead of "heterogeneous products", better use "products from heterogeneous reactions".

This has now been changed.

Reviewer 2

The paper by Bryant et al. entitled as 'Strong anthropogenic control of secondary organic aerosol formation from isoprene in Beijing' shows the observational data for isoprene-derived organic aerosol (iSOA), especially focusing on orgnaosulfate. Although observational data of iSOA in Beijing itself might be unique, the reviewer believes that the manuscript needs to be re-structured and more carefully prepared to meet the publication criteria for ACP. Discussion of the data could have been deeper and

more convincing if the authors have analyzed the data in more detail and carefully. There were numerous errors in the reference list. Some technical descriptions were not clear. I can understand that the authors have put significant effort to obtain this
dataset. So, the manuscript should have been prepared more carefully.

We thank the reviewer for their helpful comments and suggestions. However, we do not understand why they think it does not meet "ACP criteria"? We feel the paper has been written carefully and we have added clarification to the points below. When large scale field experiments are carried out, there are often numerous groups concentrating their publications on specific areas. Here we are interested in the isoprene SOA and feel that an extensive discussion of the gas phase data is not needed and can be found in Shi et al., 2019 and other subsequent research papers. However, we have added a small section to draw out the main conclusions from the auxiliary data as shown in reviewer 1 comment 2 and the new section 3.2

We could only find a few errors and one duplication in the reference list and these have been addressed.

Major comments

Major comments Figures 3 and S1. L331 'OH chemistry is still an important loss route at night (>30 %) owing to night-time OH sources, such as the ozonolysis of alkenes.' The authors estimated that the contribution of OH radicals on the loss process of isoprene is more than 50% even during nighttime, as the concentration of OH radical is close to 2 _ 106 molecules cm-3 even at around the midnight. However, this concentration
seems to be higher than OH concentrations in other urban areas during nighttime (Kanaya et al., 2007;Heard et al., 2004). Although I am not familiar with other recent field campaigns for OH radicals in Beijing, a recent modeling result also indicated that OH radical concentration in Beijing should be orders of magnitudes lower
than what the authors have reported (Tan et al., 2019). If the night-time OH sources in Beijing is so important for isoprene oxidation chemistry, the potential sources need to be discussed in more detail by employing observation data or by appropriately citing necessary publications.

Actually, significant OH concentrations have been seen at night for field campaigns performed in both the Beijing and Pearl River Delta areas in China. In Lu at el. (ACP 2014) OH concentrations of up to $3x10^6$ at night (higher than those reported for our work at night) were observed and there is a modelling study of two campaigns in that paper which discusses radical sources at night, and it was proposed that these levels can be reconciled if the model includes an additional ROx production process. A further discussion of night-time chemistry is out of scope of the current paper, there are other papers in preparation which will discuss night-time radical chemistry in more detail. We have added Lu et al. as a reference to potential sources of OH and other radicals at night in this type of environment in China."

Lu, K. D., Rohrer, F., Holland, F., Fuchs, H., Brauers, T., Oebel, A., Dlugi, R., Hu, M., Li, X., Lou, S. R., Shao, M., Zhu, T., Wahner, A., Zhang, Y. H., and Hofzumahaus, A.: Nighttime observation and chemistry of HOx in the Pearl River Delta and Beijing in summer 2006, Atmos. Chem. Phys., 14, 4979–4999, https://doi.org/10.5194/acp-14-4979-2014, 2014.

L421 'The correlation of [O3] [pSO4] '/Figure 5 It seems to me that the authors have assumed that the formation of organosulfate is approximated by the second order reaction with a constant reaction rate. However, it is a multiphase chemistry. In addition, the importance of particle phase acidity and phase are known to influence the rate of such chemical reactions. So, I am not sure if it is a good idea to assume that the
rate constant is a fixed value. Figure 4 indicates that the concentrations of all the organosulfates are high during pollution episodes. Although the authors did not provide time-series data for sulfate concentration, I speculate that it must have also been high during these time periods. Considering that the ozone concentration was less
variable than particle phase species (Figure 1), I suspect that the correlation shown in Figure 5 is dominantly driven by accumulation of particle phase species (i.e., sulfate and organosulfate) during pollution episodes, although there must have also been insitu production of these species. The discussion will need to be thoroughly revised, including reconsideration of the metric.

We disagree with the reviewers comments here. The correlation between the OS and particulate sulfate is weaker than the correlation with [O3][SO4] as shown in figure S10 (now the new Figure 5). We are not suggesting there is a direct reaction with a fixed rate constant under all conditions, but at this location ozone is acting as a proxy of the photochemical oxidation of isoprene, leading to the precursors of the OS. Therefore their formation rates are dependent on the production of isoprene

oxidation products and the particle phase reaction(s) with sulfate. This relationship may not hold at longer photochemical lifetimes and under different conditions.

Other comments L300 'OH, HO2 and RO2 concentrations were measured using Fluorescence Assay by Gas Expansion (FAGE) and NO3 concentrations were measured using Broadband cavity enhanced absorption spectrometry (Zhou et al.,2018).' I checked Zhou et al. (2018); however, I was unable to find the corresponding information (maybe, I missed)?

This has been addressed. Cited Whalley et al., 2010.

L321 'There was strong a correlation between the isoprene mixing ratio measured at 8 m by the DC-GC and at 102 m using the SIFT-MS (R2 = 0.77). The SIFT-MS measurements were therefore used to investigate the correlation with iSOA tracers when no DC-GC data was available.' Being correlated does not mean that they are
quantitatively the same. Further detailed descriptions would be needed.

There was an offset in concentration between the isoprene measured at the ground and at 100 m reflecting the loss rate of isoprene during transport from surface emissions. We originally included this information and felt it was not needed. However, we have added it back in to address the reviewers comment.

Following text has been added:
L348 "The slope of the linear fit between the two data sets was 0.67, indicating a loss of around 30% of the isoprene during transport from the ground to the tower(100m)."

Section 3.3 The reviewer believes that the content is more suitable for the experimental section.

We thank the reviewer for their suggestion. However, we believe that section 3.3 should remain as part of the main text due to identifying the matrix effects as a key result of this study.

L402: 'Zero-dimensional box modelling indicates on some days up to 35 % of the isoprene-derived RO2 radicals can react with HO2 in the afternoon (Newland et al., 2019).' As Newland et al. (2019) has not been published yet, I am unable to evaluate the validity of this description.

Newland et al., 2019 has now been published in ACPD. https://www.atmos-chem-phys-discuss.net/acp-2020-35/

Acknowledgement It seems that at least one of the authors is also included in the acknowledgement.

Removed Yele Sun from Acknowledgements

References There are numerous errors. For example, names of some authors are duplicated. Information about issues/page numbers are unavailable for some references. Abbreviations for some journals are not following the standard style. Titles of some papers are missing. Some references are appearing twice (i.e., duplicate). The authors will need to carefully check the reference list again.

These have been addressed.

Figure 1 It seems that all the data points are connected by line, even if some data are missing. I suggest to change it so that the readers can tell for which time period the data is/is not available.

Addressed in previous comment to reviewer 1 and now in the new version of Figure 1.

Figure 3 (caption) What is the unit for the reaction rate constants?

Text added: "cm^3 $molecule^{-1}$ s^{-1}"

Reviewer 3

Comments:

In this work, the authors have quantified a number of organic tracers, primarily organosulfates or nitroxyorganosulfates in order to better the contribution of isoprene derived secondary organic aerosol (iSOA) to organic aerosol carbon in the atmosphere. They found that iSOA formation in urban Beijing is strongly controlled by anthropogenic emissions. This work provides new valuable field data to better understand
the sources of ambient aerosols in an urban polluted environment. I support the publication of this work in ACP and have some comments for the authors' consideration.

Comments Line 43, "The coelution of the inorganic ions in the extracts caused matrix effects that impacted two authentic standards differently." This is a very good finding. However, the authors do not further elaborate this point here. What is the potential significance of matrix effects on the quantification of the species in this work?

This has been addressed in response to reviewer one, comment 4.

Line 51, "These results indicate for the first time that iSOA formation in urban Beijing is strongly controlled by anthropogenic emissions and results in extensive conversion to heterogeneous OS products". Could the authors further elaborate the correlation between the formation of iSOA controlled by the emissions of anthropogenic pollutants and formation of OSs in a more quantitative way? How significance or any numbers
based on their field observations and data?

We have addressed this in our response to reviewer 1, comment 1.

Line 336, "This indicates that there are significant local emissions of isoprene impacting the measurement site and therefore a high potential for the formation of iSOA in this urban environment." Could the authors further comment whether the sampling site be a representative site for the typical urban environment in most parts of Beijing? Could the observations and results presented in this work largely reflect the title of this paper
"Strong anthropogenic control of secondary organic aerosol formation from isoprene in Beijing"?

The site which was located between the fourth and third north ring roads of Beijing is a largely residential area which is typical of Beijing as described in Shi et al. As such, this study is thought to be representative of Beijing as a whole. Beijing has a very high proportion of green space (55%) indicating there is significant coverage of land with plants which could emit isoprene.

Line 342, "The full list of iSOA tracers, along with their measured m/z and molecular formula is shown in Table 1, ordered by descending average concentration (weighted by filter sampling time and reported in ng m-3) during the campaign" What are the uncertainties of the reported concentrations? Please present the uncertainties.

The estimated uncertainties were discussed in section 3.4 as 60 %, accounting for the use of the matrix correction factors.

Line 360, "A strong matrix effect was observed for the 2-MT-OS, with the concentration measured by standard addition calibration 8.6 to 10 times higher than when using the external calibration carried out on the same day." This is an important finding. Why? Could the authors explain these results?

The extracted samples are a complex mixture of different compounds, including a high proportion of inorganic ions that are extracted into water. This is likely to change the surface tension of the droplet produced in the source and the ion distribution. Further work is needed to fully understand the reasons. The following text has been added:
"The matrix effects identified in this study are likely due to the extracted samples being a complex mixture of different compounds, including a high proportion of inorganic ions that are extracted into water. This is likely to change the surface tension of the droplet produced in the ionisation source and the ion distribution. Further work is needed to fully understand the reasons."

Line 404, “Zero-dimensional box modelling indicates on some days up to 35 % of the isoprene-derived RO2 radicals can react with HO2 in the afternoon (Newland et al., 2019).” Please kindly note that this paper is under review or has been accepted for publication.

Newland et al., 2019 has now been published in ACPD. https://www.atmos-chem-phys-discuss.net/acp-2020-35/

Line 425, “Therefore, these spikes in 2-MT-OS could be a result of either higher 2-MTOS in regional aerosol transported to the site or a high isoprene emission source to the south west of the site (i.e. producing IEPOX locally) that then reacts with increased regional sulfate pollution.” Any field evidences or model predictions show that the IEPOX can be effectively produced locally? What are the contributions from the regional transport? The effects of anthropogenic emission on iSOA formation observed in this work are local, regional or a combination of both effects.

We have added a sentence to clarify that the influence of anthropogenic pollutants on iSOA is occurring at both the local and regional level.

The following text has been added: “. The I-CIMS data shows that the IEPOX/ISOPOOH (Figure S5 and Newland et al., 2020) signal increases during the afternoon as the NO levels drop to below 1 ppb. The low NO levels mean that up to 30 % of the isoprene peroxy radical from OH oxidation can react with HO_2 rather than NO at this site, meaning IEPOX can be formed locally (Newland et al., 2020). There is also likely to be a regional source of IEPOX and 2-MT-OS, suggesting both local and regional anthropogenic influences.”

Line 450, “The ratio of 2-MT-OS:2-MG-OS observed in Beijing is compared to previous studies in Table 2 and is considerably lower than measurements taken in a range of isoprene dominated environments (South East US, 2-MT-OS:2-MG-OS = 17, Budisolistiorini et al., 2015.; Amazon, 2-MTOS:2-MG-OS = 13-118, Glasius et al., (2018).; Atlanta, 2-MT-OS:2-MG-OS = 33, Hettiyadura et al., (2019)) reflecting the strong impact
of urban NO emission on iSOA formation.” I agree with this argument. However, how could we use this ratio to quantify the effect of NO emission on iSOA formation or OS formation in different regions?

We like the reviewers suggestion of using this kind of data as a metric for understanding the formation pathways in different environments. However, at present there is not enough information available for the ratio of these species in urban or suburban areas to develop this metric. This has been added as a suggestion for future work.

The following text was added: “Future work will investigate how to use these ratios to quantify the effect of NO emission on iSOA formation in different regions.”

Line 505, “Some of the NOS observed peaked in the daytime and some were enhanced at night. In total they had a mean concentration of 24 ng m-3 during the campaign. The sources and formation of these species will be discussed in a separate publication.” I am okay with this. However, could the authors briefly elaborate how the detection of NOS help to better understand the effect of anthropogenic emission on the iSOA
formation in this work?

Thank you for your comment. We have added:
“NOS species are formed via the heterogenous uptake of isoprene nitrates (IN) into the particle phase. Nitrate radicals play a key role in the formation of IN, with nitrate radicals forming from reaction of NO_2 with O_3, both key anthropogenic pollutants. Therefore, emissions of NOx and formation of particulate sulfate will enhance the production of isoprene NOS species.”

Strong anthropogenic control of secondary organic aerosol formation from isoprene in Beijing

Daniel J. Bryant[1], William J. Dixon[1], James R. Hopkins[1,2], Rachel E. Dunmore[1], Kelly L. Pereira[1], Marvin Shaw[1,2], Freya A. Squires[1], Thomas J. Bannan[3], Archit Mehra[3], Stephen D. Worrall[3±], Asan Bacak[3], Hugh Coe[3], Carl J. Percival[3φ], Lisa K. Whalley[4,5], Dwayne E. Heard[4], Eloise J. Slater[4], Bin Ouyang[6,7], Tianqu Cui[8ω], Jason D. Surratt[8], Di Liu[9υ], Zongbo Shi[9,10], Roy Harrison[9], Yele Sun[11], Weiqi Xu[11], Alastair C. Lewis[1,2], James D. Lee[1,2], Andrew R. Rickard[1,2], Jacqueline F. Hamilton[1]

[1] Wolfson Atmospheric Chemistry Laboratories, Department of Chemistry, University of York, York, UK
[2] National Centre for Atmospheric Science, University of York, York, UK
[3] School of Earth and Environmental Sciences, The University of Manchester, Manchester, UK
[4] School of Chemistry, University of Leeds, Leeds, UK
[5] National Centre for Atmospheric Science, University of Leeds, Leeds, United Kingdom
[6] Lancaster Environment Centre, Lancaster University, Lancaster, UK
[7] Department of Chemistry, University of Cambridge, Cambridge, UK
[8] Department of Environmental Sciences and Engineering, Gillings School of Global Health, University of North Carolina, Chapel Hill, USA
[9] School of Geography Earth and Environmental Sciences, the University of Birmingham, Birmingham, UK
[10] Institute of Surface-Earth System Science, Tianjin University, Tianjin, China
[11] Institute of Atmospheric Physics, Chinese Academy of Sciences, Beijing, People's Republic of China

± Now at Chemical Engineering and Applied Chemistry, School of Engineering and Applied Science, Aston University, Birmingham, UK
φ Now at Jet Propulsion Laboratory, California Institute of Technology, 4800 Oak Grove Drive, Pasadena, CA, USA
ω Now at Laboratory of Atmospheric Chemistry, Paul Scherrer Institute, 5232 Villigen, Switzerland
υ Now at State Key Laboratory of Organic Geochemistry and Guangdong Provincial Key Laboratory of Environmental Protection and Resources Utilization, Guangzhou Institute of Geochemistry, Chinese Academy of Sciences, Guangzhou 510640, China

Correspondence to: Jacqueline Hamilton (jacqui.hamilton@york.ac.uk)

Abstract: Isoprene-derived secondary organic aerosol (iSOA) is a significant contributor to organic carbon (OC) in some forested regions, such as tropical rainforests and the Southeast US. However, its contribution to organic aerosol in urban areas, with high levels of anthropogenic pollutants, is poorly understood. In this study we examined the formation of anthropogenic-influenced iSOA during summer in Beijing, China. Local isoprene emissions and high levels of anthropogenic pollutants, in particular NO_X and particulate SO_4^{2-}, led to the formation of iSOA under both high- and low-NO oxidation conditions, with significant heterogeneous transformations of isoprene-derived oxidation products to particulate organosulfates (OSs) and nitrooxy-organosulfates (NOSs). Ultra-pressure liquid chromatography coupled to high-resolution mass spectrometry was combined with a rapid automated data processing technique to quantify 31 proposed iSOA tracers in offline $PM_{2.5}$ filter extracts. The co-elution of the inorganic ions in the extracts caused matrix effects that impacted two authentic standards differently. The average concentration of iSOA OSs and NOSs was 82.5 ng m^{-3}, around three times higher than the observed concentrations of their oxygenated precursors (2-methyltetrols and 2-methylglyceric acid). OS formation was dependant on both photochemistry and sulfate available for

reactive uptake as shown by a strong correlation with the product of ozone (O_3) and particulate sulfate (SO_4^{2-}). A greater proportion of high-NO OS products were observed in Beijing compared to previous studies in less polluted environments. The iSOA derived OSs and NOSs represented on average 0.62 % of the oxidised organic aerosol measured by aerosol mass spectrometry, but this increased to ~3 % on certain days. These results indicate for the first time that iSOA formation in urban Beijing is strongly controlled by anthropogenic emissions and results in extensive conversion to OS products from heterogenous reactions.

1 Introduction

Rapidly developing countries such as China often experience very poor air quality. Beijing regularly experiences periods of very high particle pollution, with annual and 24-hourly levels well above World Health Organisation guidelines (Chan et al., 2008; Hu et al., 2014). Premature mortality, as a result of respiratory illness, cardiovascular disease and cancer, has been associated with exposure to poor air quality (Dockery et al., 1993; Pope et al., 2000, 2006; Jerrett et al., 2009; Beelen et al., 2014; Laurent et al., 2014; Ostro et al., 2015). Lelieveld et al. (2015) estimated that 1.36 million premature deaths in China in 2010 were a result of exposure to outdoor air pollution. By far the most dangerous pollutant to health in China are particles less than 2.5 microns in diameter, known as $PM_{2.5}$, with a recent study suggesting that a 50 % reduction in excess mortality requires a 62 % reduction in $PM_{2.5}$ in the Beijing-Tianjin-Hebei (BTH) region (Hu et al., 2017a).

Previous measurements using aerosol mass spectrometry (AMS) indicate that PM_1 in Beijing is mainly composed of sulfate, nitrate, ammonium and organics (Hu et al., 2016. Zhang et al., 2013). Positive Matrix Factorisation of AMS measurements indicate that oxidised or secondary organic aerosol (SOA) can make up a substantial fraction of the PM_1 mass (> 25 %), even in urban areas, but the sources of this material are still poorly understood (Zhang et al., 2011; Sun et al., 2018). Hu et al. (2017a) estimated that exposure to SOA was responsible for 0.14 million deaths in China in 2013 based on mass contribution alone, ranging from < 1 % to 23 % source contributions to $PM_{2.5}$ depending on location. Zhang et al. (2017) used ^{14}C measurements to determine that non-fossil emissions are generally a dominant contributor of secondary organic carbon (SOC) in Beijing, with a larger contribution in summer as a result of increased biogenic volatile organic compounds (VOCs) emissions.

Hu et al. (2017b) updated the Community Multi-scale Air Quality (CMAQ) model with updated SOA yields and a more detailed description of SOA formation from isoprene oxidation. Removing all anthropogenic pollutants from the model resulted in a huge drop in isoprene SOA concentrations, indicating that controlling anthropogenic emissions would result in reduction of both anthropogenic and biogenic SOA. The predicted SOA was dominated by isoprene in summer across China and in four cities (Beijing, Guangzhou, Shanghai, Chengdu) with concentrations up to 30 μg m^{-3} in Beijing. However, there is currently very little observational evidence to support such high SOA mass concentrations from isoprene oxidation in these Chinese cities. The widely used SOA tracer method (Kleindienst et al., 2007) has been used extensively to estimate the fraction of isoprene-derived SOA (iSOA) across China. Ding

et al. (2014) studied SOA at 14 Chinese sites and found that iSOA dominated the apportioned SOA mass (46 ± 14 %), with it contributing between 0.4 – 2.17 μg m^{-3} and an average of 1.59 μg m^{-3} in Beijing. However, only a very limited subset of VOC precursors was included, and this method fails to account for heterogeneous formation processes. To overcome some of these limitations, Wang et al. (2017) used tracer-based source apportionment of $PM_{2.5}$ with positive matrix factorisation in the Pearl River Delta region during summer. They identified an iSOA factor that contributed up to 4 μg m^{-3} in Guangzhou, and up to 11 % of the total SOC.

A multitude of studies have examined iSOA formation (Pandis et al., 1991; Edney et al., 2005; Kroll et al., 2006; Dommen et al., 2006; Kleindienst et al., 2006; Ng et al., 2006; Surratt et al., 2007a, 2007b, 2008, 2010; Ng et al., 2008; Paulot et al., 2009; Chan et al., 2010; Chhabra et al., 2010; Nguyen et al., 2011, 2014, 2015; Zhang et al., 2011, 2012; Lin et al., 2013; Xu et al., 2014; Krechmer et al., 2015; Clark et al., 2016; Riva et al., 2016a, 2016b); however, the magnitude of iSOA formed can be vastly different from study to study (Carlton et al., 2009). Furthermore, there have been limited field measurements to establish if these estimates are representative of urban environments (Wang et al., 2018; Li et al., 2018; Glasius et al., 2018; Le Breton et al., 2018; Hettiyadura et al., 2018,2019; Rattanavaraha et al., 2016; Budisulistiorini et al., 2013).

iSOA formation during the daytime is dominated by reaction with hydroxyl radicals (OH), with the concentrations of NO having a strong influence on the reaction products (Wennberg et al., 2018 and references therein). Under low-NO conditions the isoprene peroxyradicals (RO_2) can react with hydroperoxy radicals (HO_2) to form isoprene hydroxyhydroperoxides (ISOPOOH). The ISOPOOH isomers can react further with OH to form isoprene epoxydiol isomers (β− or δ-IEPOX) (Paulot et al., 2009), which can undergo uptake into acidified sulfate particles to form 2-methyltetrol organosulfates (2-MT-OS) (Surratt et al., 2010. Lin et al., 2012). Under high-NO conditions, isoprene RO_2 can react with NO to form alkoxy radicals (RO) producing methacrolein (MACR) and methyl vinyl ketone (MVK) as the main reaction products. The reaction of MACR with OH, and subsequent addition of NO_2, leads to the methylacrloylperoxynitrate (MPAN), which reacts with OH to produce hydroxymethylmethyl-α-lactone (HMML) (Nguyen et al., 2015) or methyacrylic epoxide (MAE) (Lin et al., 2013). HMML is thought to be the more abundant product compared to MAE (Nguyen et al., 2015). Subsequent uptake of HMML into wet sulfate aerosols is proposed to lead to either 2-methylglyceric acid (2-MG) or its organosulfate derivative (2-MG-OS), as well as their dimers and higher order oligomers (Surratt et al., 2006; Surratt et al., 2010; Lin et al., 2013; Nguyen et al., 2015). Recently Schwantes et al. (2019) showed that under ambient conditions the formation of SOA from low-volatility nitrates and dinitrates, formed via reactions of isoprene derived RO_2 with NO, is also important. Chamber-derived SOA yields for OH chemistry are variable depending on the experimental conditions, but are generally low (<10 %). The addition of acidified sulfate aerosol, accounting for wall losses and using more atmospherically relevant radical lifetimes can lead to significantly higher SOA yields in chamber studies (Surratt et al., 2010; Lin et al. 2012; Gaston et al., 2014). However, recent work has revealed that isoprene SOA formation can be suppressed when viscous organic coatings are present on acidified sulfate aerosol, impeding the

multiphase chemistry of IEPOX yielding additional SOA (Riva et al., 2016b; Zhang et al., 2018; Riva et al., 2019).

Observations using aerosol mass spectrometry (AMS) indicate that IEPOX-derived SOA can make up a significant fraction of organic aerosol in isoprene-rich environments, such as Borneo (23 %; Robinson et al., 2011), the Amazon (34 %; Chen et al., 2015) and the South East US (33-40 %; Budisulistiorini et al., 2013; Budisulistiorini et al., 2016; Rattanvaraha et al., 2017). Hu et al. (2015) compared previous AMS studies and found a magnitude lower average IEPOX-SOA signal in urban studies (f_{C5H6O} = 0.17 %) compared to those in isoprene-rich regions (f_{C5H6O} = 2.2 %). The average IEPOX-SOA concentration measured in Nanjing, a polluted city in Eastern China, in August 2013 was 0.33 μg m^{-3} (Zhang et al., 2017). This represented only 3.8 % of the total OA, indicating there is limited formation of IEPOX under high-NO_x conditions (average NO_x = 21 ppb). He et al. (2018) found higher concentrations of the low-NO isoprene SOA tracers (average = 121 ng m^{-3}) than the high-NO iSOA tracers (average = 9 ng m^{-3}) at a regional background site (Wanqingsha) situated within the heavily polluted Pearl River Delta Region. Only two high-NO iSOA tracers were measured (2-MG and 2-MG-OS), which could lead to a significant underestimate of the strength of the high NO_x pathway. Wang et al. (2018) measured a range of OSs at a regional site 38 km north east of Beijing during May-June 2016. Isoprene-derived OSs ranged from 0.9-20 ng m^{-3}, with a mean isoprene-derived OS concentration of 14.8 ng m^{-3}. In both these studies, the ratio of the average concentration of the commonly used OS tracers from the low NO versus the high NO pathways was close to 1.5 (2-MT-OS:2-MG-OS; Beijing = 1.47, Wanqingsha = 1.57) indicating that even in polluted environments low-NO oxidation chemistry can play a significant role in iSOA formation.

SOA formed from anthropogenic and other biogenic (monoterpenes and sesquiterpenes) sources have also been studied. Thousands of organic species including hundreds of OS and nitroxy OS (NOS) species have been identified studies from a range of precursors using UPLC/ESI-HR-MS from ambient aerosol samples (Wang et al., 2016, Wang et al., 2017). Brüggemann et al. (2019) quantified with authentic standards both monoterpene OS (MT-OS) and sesquiterpene OS (SQT-OS) species in Melpitz, Germany and Wangdu, China. They found median daytime concentrations for Melpitz and Wangdu for 52 MT-OS species of 12.15 ng m^{-3} and 38.19 ng m^{-3} respectively. For the 5 SQT-OS species, median concentrations were 0.3 ng m^{-3} and 3.90 ng m^{-3} for daytime concentrations respectively, much lower than the iSOA OS species quantified in this study. Riva et al. (2016) identified OS species from the photo-oxidation of C_{10} – C_{12} alkanes, which were then characterised in ambient aerosol samples collected in Lahore, Pakistan and Pasadena, CA, USA. High concentrations of OS species were identified in Lahore, with the largest observed concentration arising from a cycodecane OS species ($C_{10}H_{16}O_7S$) with a concentration of 35.93 ng m^{-3}.

The lack of molecular-level measurements of iSOA in highly polluted urban areas makes it difficult to determine the role of isoprene in summer haze episodes in Beijing. To investigate the formation of iSOA in Beijing, offline $PM_{2.5}$ filter samples were collected during summer 2017 as part of the Atmospheric

Pollution and Human Health program (Shi et al., 2019). The filters were extracted and then screened using a sensitive and selective high throughput method based on ultra-performance liquid chromatography coupled to ultra-high-resolution mass spectrometry equipped with electrospray ionization (UPLC/ESI-HR-MS). High-time resolution filter sampling allowed the formation and evolution of iSOA to be studied, with observed concentrations strongly controlled by levels of anthropogenic pollutants.

2 Experimental

2.1 $PM_{2.5}$ filter sampling and extraction

Aerosol samples were collected between the 18th May and 24th June 2017 at the Institute of Atmospheric Physics (IAP) in Beijing, China. This sampling was part of the Sources and Emissions of Air Pollutants in Beijing (AIRPOLL-Beijing) project, as part of the wider Atmospheric Pollution and Human Health in a Chinese Megacity (APHH-Beijing) programme (Shi et al., 2019). $PM_{2.5}$ filter samples were collected using an ECOTECH HiVol 3000 (Ecotech, Australia) high-volume air sampler with a selective $PM_{2.5}$ inlet, with a flow rate of 1.33 m^3 min^{-1}. Filters were baked at 500 °C for five hours before use. After collection, samples were wrapped in foil, and then stored at -20 °C and shipped to the laboratory for offline analysis. Samples were collected at a height of 8 m, on top of a building in the IAP complex. Samples were collected every 3 hours during the day, approximately between 08:30 and 17:30 and then one sample was collected overnight between 17:30 and 08:30. Hourly samples were also taken on certain days towards the end of the sampling period on high pollution days. 24-hour samples were also collected using a Digitel high volume $PM_{2.5}$ sampler at the same location.

The extraction of the organic aerosol from the filter samples was based on the method in Hamilton et al., (2008). Initially, an 8th of the filter was cut up into roughly 1 cm^2 pieces and stored in a vial. 4 ml of LC-MS grade H_2O was then added to the sample and left for two hours. The samples were then sonicated for 30 minutes. A small subset (3) of the filter samples were also extracted via orbital shaker and no appreciable difference was found in the concentrations of the iSOA tracers compared to sonication. Using a 2 ml syringe, the water extract is then pushed through a 0.22 μm filter (Millipore) into another sample vial. An additional 1 mL of water was added to the filter sample, then extracted through the filter, to give a combined aqueous extract. This extract was then reduced to dryness using a vacuum solvent evaporator (Biotage, Sweden). The dry sample was then reconstituted in 1 mL 50:50 MeOH:H_2O solution for offline chemical analysis.

2.2 Ultra-performance liquid chromatography tandem mass spectrometry (UPLC-MS^2)

~~The extracted filter samples and standards were analysed~~ The water-soluble fraction of the filter samples were analysed using ~~UPLC-MS^2~~ UPLC-full scan-ddMS^2, using an Ultimate 3000 UPLC (Thermo Scientific, USA) coupled to a Q-Exactive Orbitrap MS (Thermo Fisher Scientific, USA) with a heated electrospray ionisation (HESI). The UPLC method uses a reverse phase 5 μm, 4.6 x 100mm, Accucore column (Thermo Scientific, UK) held at 40 °C. The mobile phase consists of LC-MS grade water and 100 % MeOH (Fisher Chemical, USA). The water was acidified using 0.1 % formic acid to improve peak

resolution. The injection volume was 2 µL. The solvent gradient was held for a minute at 90:10 H_2O:MeOH, then changed linearly to 10:90 H_2O:MeOH over 9 minutes, then held for 2 minutes at this gradient before returning to 90:10 H_2O:MeOH over 2 minutes and then held at 90:10 for the remaining 2 minutes, with a flow rate of 300 µL min^{-1}. Due to the wide range of compounds studied, poor retention was observed for some species (RT < 0.8min). These species closely eluted to the dead time of the column where inorganic sulfate ions eluted (0.67 min). To check for ionisation artefacts, a aqueous solution containing 20 ppm ammonium sulfate, 1ppm 2-methytetrol and 1ppm 2-methylglyceric acid was ran under the same conditions as the filter samples to check for organosulfate formation (2-MT-OS and 2-MG-OS respectively). No MG-OS formation was observed and <0.5% conversion was seen for the 2-MT. The mass spectrometer was operated in negative mode using full scan $ddMS^2$. The scan range was set between 50 - 750 m/z, with a resolution of 70,000. The ESI voltage was 4 kV, with capillary and auxiliary gas temperatures of 320 °C. The number of most abundant precursors for MS^2 fragmentation per scan was set to 10. The samples were run in batches of 70, in a repeating sequence of 5 samples followed by one blank, each filter sample was run only once. The calibrations were run separately after the samples were finished, in the following sequence; (3 X same concentration) X number of standards in calibration curve from the lowest concentration to the highest followed by 2 blanks. The quantification method will be discussed in the results section (3.3).

2.3 Construction of accurate mass library

A mass spectral library was built using the compound database function in TraceFinder 4.1 General Quan software (Thermo Fisher Scientific, USA). Each compound was input into the compound library in the generic form: $C_cH_hO_oN_nS_s$ (where c, h, o, n, and s represent the number of carbon, hydrogen, oxygen, nitrogen and sulfur atoms respectively). From literature, species were identified, searched for in the ambient samples according to their accurate mass, and then the retention time (RT) of each isomer was obtained. Using previously observed iSOA products from literature, extracted ion chromatograms were plotted for each *m/z* value from a small subset of ambient samples and the retention time (RT) of observed species/isomer were obtained. For most of the OS species in this study the separation was not good enough to see individual isomers and only one peak was observed, which was added to the library. For the NOS species, individual isomers could be resolved, and each isomer was added to the library based on its retention time. The accurate masses, RT and literature references for iSOA tracers are shown in Table ~~1~~2.

2.4 Automated method for SOA tracer analysis

The UPLC/ESI-HR-MS data for each ambient sample and standard was analysed using TraceFinder™. Tracefinder extracted the OS/NOS tracer peak areas from each ambient sample chromatogram using the library based on RT and accurate mass. The mass tolerance of the method was set to 2 ppm and the retention time window was set to 30 s, although for species with multiple isomers present, the integration was checked to make sure the same peaks were not being integrated twice, and the window changed accordingly. The peak tailing factor was set to 2.0 to reduce the integration of the peak tails. The minimum signal to noise (S/N) for a positive identification was set to 3.0. Using the output from

TraceFinder, an *in-house* R code script was developed to combine the identified species and peak areas with the correct filter sampling date/time midpoint and volume of air sampled. Calibration curves from the standards were then obtained (as discussed in section 3.3), and the intercept and gradient inputted to quantify the iSOA tracer concentrations in the extract. These quantified values were then converted to the mass on the whole filter and divided by the volume of air sampled for that filter sampling period and converted to units of ng m^{-3}. Higher time resolution data were averaged to the filter sampling times. It should be noted that MS^2 was used to check that the iSOA species fragmented to give typical OS fragment ions.

2.5 Hydrophilic Liquid Interaction Chromatography (HILIC).

A subset of filters (n=15) were also analysed at the University of North Carolina (UNC) using a newly developed HILIC method interfaced to high-resolution quadrupole time-of-flight mass spectrometry equipped with ESI (i.e., HILIC/ESI-HR-QTOFMS) (Cui et al., 2018). Briefly, filters were extracted with 22 mL of LC/MS-grade methanol by 45 min of sonication; the samples were first extracted for 23 min, the water bath replaced with cool water, and then extracted again for 22 min. This was done to make sure the water bath contained within the sonicator did not reach above 30 C. Extracts were filtered through polypropylene membrane syringe filters in order to remove insoluble filter fibres and soot particles. The extracts were dried under a gentle stream of nitrogen gas. Dried methanol extracts were reconstituted with 150 μL of 95:5 (v/v) LC/MS-grade acetonitrile/Milli-Q water. Operating details of the HILIC/ESI-HR-QTOFMS used for these samples is also summarized by Cui et al. (2018).

2.6 Gas Chromatography – Mass Spectrometer

Details of the measurement procedure used can be found elsewhere (Fu et al., 2010). Briefly, filter samples were extracted with dichloromethane/methanol (2:1 v/v), filtered through quartz wool packed in a Pasteur pipette, concentrated using a rotary evaporator under vacuum, and blown down to dryness with pure nitrogen gas. The extracts were derivatized and diluted with n-hexane containing the internal standard prior to GC-MS analysis. Separation was performed on a fused silica capillary column (DB-5MS: 30 m × 0.25 mm × 0.25 μm). The MS detection was conducted in electron ionization (EI) mode at 70 eV, scanning from 50 to 650 Da. Individual compounds were identified by comparison of mass spectra with those of authentic standards or literature data. 2-methylglyceric acid, C_5-alkene triols (the sum of *cis*-2-methyl-1,3,4-trihydroxy-1-butene, *trans*-2-methyl-1,3,4-trihydroxy-1-butene, and 3-methyl-2,3,4-trihydroxy-1-butene), and 2-methyltetrols (the sum of 2-methylthreitol and 2-methylerythritol) were quantified using the response factor of *meso*-erythritol. Field blank filters were treated as the real samples for quality assurance. Target compounds were not detected in the blanks.

2.7 High-Resolution Aerosol Mass Spectrometry measurements

The size-resolved non-refractory submicron aerosol species at the same site were measured by an Aerodyne high-resolution time-of-flight aerosol mass spectrometer (HR-ToF-AMS) at a time resolution of 5 min. The elemental ratios of hydrogen-to-carbon (H:C) and oxygen-to-carbon (O:C) of OA were determined, and the sources of OA were analysed with positive matrix factorisation. Six OA factors were

identified in summer including two primary factors; hydrocarbon like OA (HOA), cooking OA (COA), and three oxidised OA factors with increasing degrees of oxidation, OOA1 (O:C = 0.53), OOA2 (O:C = 0.74), OOA3 (O:C = 1.18).

2.8 Iodide CIMS

A time of flight chemical ionisation mass spectrometer (ToF-CIMS) (Lee et al. 2014; Priestley et al. 2018) using an iodide ionisation system coupled with a filter inlet for gases and aerosols (FIGAERO) was deployed here to make near simultaneous, real-time measurements of both the gas- and particle-phase chemical composition. The instrument was originally developed by Lopez-Hilfiker et al. (2014) and is described and characterised in more detail by Bannan et al., (2019). The experimental set up employed by the University of Manchester ToF-CIMS is described in Zhou et al., (2019). Only gas phase data is presented herein.

Field calibrations were regularly carried out using known concentration of formic acid in gas mixtures made in a custom-made gas phase manifold. A range of other species were calibrated for after the campaign, and relative calibration factors were derived using the measured formic acid sensitivity during the in-situ calibrations (Bannan et al. 2015). Offline calibrations after the field work campaign were performed specific to the isoprene oxidation species observed here. IEPOX ($C_5H_{10}O_3$) synthesized by the University of North Carolina, Department of Environmental Sciences & Engineering was specifically calibrated for. Known concentrations were deposited on the FIGAERO filter in various amounts and thermally desorbed using a known continuous flow of nitrogen over the filter. For the isoprene nitrate; $C_5H_9NO_4$ there was no direct calibration source available and concentrations using the calibration factor of $C_5H_{10}O_3$ are presented here.

2.9 Gas-phase measurements

Additional gas-phase measurements were collected at the site from an elevated inlet at 8 m. Data included Nitrogen oxide, NO, measured by chemiluminescence with a Thermo Scientific Model 42i NO_x analyser and Nitrogen dioxide, NO_2, was measured using a Teledyne Model T500U Cavity Attenuated Phase Shift (CAPS) spectrometer. The sum of the NO_y species was measured using a Thermo Scientific Model 42C NO_x analyser and a heated molybdenum converter at the sample inlet. The molybdenum converter reduces NO_y compounds to NO allowing measurement by chemiluminescence. Ozone, O_3, was measured using a Thermo Scientific Model 49i UV photometric analyser. All instruments were calibrated throughout the measurement period, with a 'zero' or 'background' calibration using a Sofnofil/charcoal trap. Span (high concentration) calibrations were carried out using gas standards. Both the Thermo Scientific 42i and 42C instrument calibrations are traceable to the National Physical Laboratories (NPL) NO scale. The meteorological variables of wind speed, wind direction, relative humidity (RH), and temperature were measured at 102 m on the IAP 325 m meteorological tower.

Observations of VOCs were made using a dual-channel GC with flame ionisation detectors (DC-GC-FID). Air was sampled at 30 L min^{-1} at a height of 5m, through a stainless-steel manifold (½" internal diameter). 500 mL subsamples were taken, dried using a glass condensation finger held at -40°C and then pre-concentrated using a Markes Unity2 pre-concentrator on a multi-bed Ozone Precursor adsorbent trap (Markes International Ltd). These samples were then transferred to the GC over for analysis following methods described by Hopkins et al. (2011).

Further details of the following additional gas phase instrumentation can be found in the SI and Shi et al., 2019. Isoprene was also measured at a height of ~102 m using a Voice200 Selected ion flow tube mass spectrometer (SIFT-MS, Syft Technologies, Christchurch, New Zealand). OH, HO_2 and RO_2 concentrations were measured using Fluorescence Assay by Gas Expansion (FAGE) (Whalley et al., 2010) and NO_3 concentrations were measured using Broadband cavity enhanced absorption spectrometry (Le Breton et al., 2014). ~~(Zhou et al.,2018)~~

3 Results and discussion

The field campaign was conducted at the Institute of Physics, Beijing, situated between the third and fourth ring roads (Shi et al., 2019). The site is typical of central Beijing, surrounded by residential and commercial properties and is near several busy roads. It is also close to several green spaces including a tree-lined canal to the south and the Olympic forest park to the north-east, providing sources for local isoprene emissions.

3. 1 Isoprene gas phase concentrations and loss processes

Isoprene was measured hourly using the DC-GC-FID between 18/05/2017 – 20/06/2017 and the observed concentrations are shown in Figure 1, alongside NO, NO_2 and ozone. The mean mixing ratio of isoprene was 0.53 ppb, with a maximum of 2.9 ppb on the 16/06/2017. The ambient temperature ranged from 16 to 38 °C. Day-time isoprene mixing ratios increased with temperature, with all isoprene mixing ratios above 1 ppb occurring when the temperature was > 25 °C. The average diurnal profile of isoprene in Figure ~~2~~3a shows low values overnight (< 50 ppt), with a rapid increase at 6 am reaching a maximum of around 1 ppb by the afternoon. The mixing ratio rapidly decreased after 18:00 and returned to very low values by around 22:00. There was strong a correlation between the isoprene mixing ratio measured at 8 m by the DC-GC and at 102 m using the SIFT-MS (R^2 = 0.77). The SIFT-MS measurements were therefore used to investigate the correlation with iSOA tracers when no DC-GC data was available. The slope of the linear fit between the two data sets was 0.67, indicating a loss of around 30% of the isoprene during transport from the ground to the tower (100m).

Using the average observed diurnal profiles of the main atmospheric oxidants, OH, ozone and NO_3 (shown in SI Figure S1), and isoprene (Figure ~~2~~3a), the isoprene loss rate was calculated (rate of loss = k_{ox}[Oxidant][Isoprene]) and is shown in Figure ~~3~~4a. The IUPAC rate constants that were used in the calculation for NO_3, O_3 and OH were $7x10^{-13}$, $1.27x10^{17}$, $1x10^{10}$ cm^3 $molecule^{-1}$ s^{-1} respectively. The percentage contribution of each oxidant to the average diurnal isoprene loss rate is shown in Figure ~~3~~4b. During the day, OH is responsible for over 90 % of isoprene loss, with NO_3 becoming relatively more

important from 18:00 until around 03:00, although the amount of isoprene available to react rapidly decreased during this time period. OH chemistry is still an important loss route at night (>30 %) owing to night-time OH sources, such as the ozonolysis of alkenes (Lu et al., 2014). Loss of isoprene via ozonolysis however is a minor route, contributing <15 %. During the daytime (10:00-15:00), the lifetime of isoprene was on average around 20 minutes, increasing to a maximum of around 6 hours at 03:00. While the high levels of oxidants lead to a short isoprene lifetime during the day, the ambient concentrations of isoprene are still maintained at the ppb level. This indicates that there are significant local emissions of isoprene impacting the measurement site and therefore a high potential for the formation of iSOA in this urban environment.

3.2 Anthropogenic tracers

A range of gas phase anthropogenic tracers were measured during the campaign as discussed in Shi et al., 2019. Figure 1 shows the time series of NO, NO_2, O_3 and particulate sulfate during the part of the campaign analysed in this study. Table 1 shows the average, maximum and minimum concentrations for these anthropogenic pollutants. NO mixing ratios ranged from less than 10.1 ppbv to 104 ppbv, and a mean concentration during the filter sampling period of 5.1 ppb. The highest concentrations generally occurred in the morning 04:00-07:00 and steadily decreased during the day. On some days, the mixing ratio of NO was very low in the afternoon, as a result of reaction with ozone and other unknown sinks (Newland et al., 2020). The mean mixing ratio of NO_2 was 22.3 ppbV, much higher than NO, with a range of 3.7 to 95 ppbv. NO_2 peaked between 06:00-07:00 and decreased to a minima at 14:00 and then steady increased until about 20:00. High afternoon concentrations of O_3 (>80 ppb) were found on most days, with a maximum observed mixing ratio of 182 ppbv. Night time O_3 levels were much lower due to reduced photochemistry and reaction with NO, although on some nights O_3 levels were maintained above 40 ppbv, as shown in Figure 1. particulate sulfate concentrations, measured by AMS are also shown in figure 1. Sulfate ranged from 0.7 to 21.7 μg m^{-3}, with an average of 5.5 μg m^{-3}. The time series shows a number of periods of high sulfate concentrations and these generally matched periods of increased $PM_{2.5}$ (see figure 9). Figure 2 shows the wind direction dependent concentrations of particulate sulfate for the sampling period in a pollutionRose plot (Openair package, R). There is a strong source of sulfate from the south of the sampling site, which is enhanced under the highest wind speeds. Previous studies have shown a strong source of pollution from the south west of Beijing, which is where many industrial factories are located (Wang et al., 2005).

~~3.2~~ 3.3 Isoprene SOA in Beijing

Using the high throughput screening method described, the peak areas of 31 potential isoprene-derived OSs and NOSs, which are known iSOA tracers, were measured in 132 $PM_{2.5}$ filter extracts. The full list of iSOA tracers, along with their measured *m/z* and molecular formula is shown in Table ~~1~~2, ordered by descending average concentration (weighted by filter sampling time and reported in ng m^{-3}) during the

campaign. The isoprene SOA tracers identified in this study are correlated towards themselves as well as common anthropogenic tracers in a corplot (Openair, R), shown in Figure 5. The corplot highlights the correlations of the iSOA tracers to each other as well as the moderate to strong correlations towards some of the anthropogenic pollutants as discussed in further sections.

~~3.3~~ 3.4 Quantification of isoprene OS tracers

Initially, two synthesised isoprene-derived OS standards (2-MT-OS and 2-MG-OS, Cui et al., 2018; Rattanavaraha et al., 2016) were used to produce calibration curves. Both standards gave strong linear calibration curves (R^2 = 0.980 and 0.996 respectively) across an appropriate range of concentrations for the peak areas in the samples. The gradient obtained for the 2-MT-OS standard was ~4 times higher than that of the 2-MG-OS, as shown in Figure S2. To investigate the potential for matrix effects from the large amounts of inorganic sulfate, nitrate and other particulate components that co-elute due to the poor retention of OS in reverse phase UPLC, standard addition calibrations were used. Five-point standard addition calibrations were run on 6 different filter extracts, covering both day and night-time, samples, during periods of both high and low concentrations of iSOA species. This therefore gives a representative sample of filters for the entire sampling period. 50 µL of filter sample extract and 50 µL of the calibrant solution were combined, giving a dilution factor of 2. The five-point calibration range of standard added to each sample was between 0-3 ppm for 2-MGOS and 0-1 ppm for 2-MT-OS. Two examples of the standard addition calibrations are shown in SI Figures S3 (2-MG-OS) and S4 (2-MT-OS), with good linear fits observed (R^2 = 0.997 and 0.997 respectively). A strong matrix effect was observed for the 2-MT-OS, with the concentration measured by standard addition calibration 8.6 to 10 times higher than when using the external calibration carried out on the same day. In contrast, the 2-MG-OS showed a much lower matrix effect, with the concentrations only 1.1-1.5 times higher when using the standard addition calibration. A further comparison using camphorsulfonate, which has a longer retention time (3.74 min) and so does not experience high inorganic ion concentrations in the source, showed no matrix effects when using standard addition. ~~Tables 1 and 2~~ Tables S1 and S2 shows a comparison of the concentrations calculated from the standard additions and the two external calibrations. Table S1 shows the concentration of 2-MT-OS in three filter sample extracts (144, 204, 208) calculated via standard addition of 2-MT-OS to the filter sample extract and via external calibrations using both 2-MT-OS and 2-MG-OS. The ratio of the standard addition to the external calibrations then gives an estimate of the under or overestimate the external calibrations make to calculating the concentration of 2-MT-OS in the samples. Both the external calibrations would lead to an underestimation of concentration of 2-MT-OS in the filter samples. 2-MG-OS provided a closer quantification of 2-MT-OS in the samples, with an average factor of 2.3 underestimation, while the 2-MT-OS external calibration gives a sample concentration a factor of 10 lower than the standard addition determined concentration.

It is not realistic to carry out standard addition calibrations for all samples and all SOA tracers. When the 2-MG-OS external calibration was used to predict the 2-MT-OS concentrations during the standard addition experiments, the concentrations were within a factor of 1.5-2.5. Therefore, the 2-MG-OS external calibration was used as a proxy for all isoprene SOA tracers, with scaling factors applied to account for matrix effects (1.33 for 2-MG-OS, 2.33 for 2-MT-OS, and an average of 1.83 used for all

other OSs). Therefore, we estimate an uncertainty on our measured concentrations of 60%, this uncertainty was calculated to account for the difference in the measured correction factors used when correcting for the matrix effects. The matrix effects identified in this study are likely due to the extracted samples being a complex mixture of different compounds, including a high proportion of inorganic ions that are extracted into water. This is likely to change the surface tension of the droplet produced in the ionisation source and the ion distribution. Further work is needed to fully understand the reasons. Without these additional standard addition calibrations, the iSOA concentrations would have been largely underestimated. The dinitrate and trinitrate NOS species eluted after the sulfate peak (R_t >1.6 min). In the absence of authentic standards for these species, camphorsulfonic acid was used as a proxy for calibration. This work highlights an additional difficulty of calibration when using ESI-MS to study OSs and indicates that future studies using reversed phase LC (RPLC) should consider the impacts of matrix effects.

~~3.4~~3.5 Organosulfates

~~3.4~~3.5.1 2-methyltetrol OS (2-MT-OS)

The 2-MT-OS ($C_5H_{12}SO_7$) formed from the uptake of IEPOX into the particle phase is often used as a marker of low-NO isoprene photochemistry (Wennberg et al., 2018). The time series of 2-MT-OS is shown in Figure ~~4~~6a. The particle concentration ranged from 0.7 ng m^{-3} to a maximum of 111 ng m^{-3}, with a mean concentration of 11.8 ng m^{-3}. The mean concentrations of 2-MT-OS and 2-MG-OS are compared to observations in previous studies in Table ~~2~~3. The mean concentration observed in Beijing was much lower than those observed in the Amazon (Riva et al., 2019) and the SE US (Budisolistiorini et al., 2015; Hettiyadura et al., 2019) but are higher than summer time observations at polluted regional sites in China (Wang et al., 2018; He et al., 2018). The lower amounts of IEPOX-derived SOA results in an average AMS f_{C5H6O} in Beijing during the APHH project of only 0.2 %, similar to observations in other urban studies (Hu et al., 2015).

Hourly samples were collected on selected high pollution days and used to obtain information on the diurnal evolution of the iSOA tracers. The findings on these days are consistent with the three-hourly data. The particulate 2-MT-OS measured by UPLC-MS, on the 11th - 12th June 2017, had a strong diurnal profile (Figure ~~2~~3b), peaking in the late afternoon, between 15:30 and 18:30, with a minimum over-night. This is consistent with the average diurnal profile of the gas phase precursors IEPOX+ISOPOOH ($C_5H_{12}O_3$) measured using the I^--CIMS (SI Figure S5). High levels of ozone were observed in the afternoon (up to 180 ppb), leading to relatively low levels of NO observed for a highly polluted environment, in some cases below 500 ppt. Thus, although the mixing ratio of NO_x was high, on most afternoons less than 2 % was in the form of NO. High levels of peroxy radicals were observed, with mean afternoon concentrations of HO_2 and RO_2 of around 3 x 10^8 molecule cm^{-3} and 1.5 x 10^9 molecule cm^{-3}, respectively. Zero-dimensional box modelling indicates on some days up to 35 % of the isoprene-derived RO_2 radicals can react with HO_2 in the afternoon (Newland et al., 2019). Thus, the diurnal profile seen in Figure ~~2~~3b, measured in samples during the measurement period suggests that IEPOX was formed at this urban location by the reaction of OH with local isoprene emissions, with a fraction of the RO_2

radicals formed reacting with HO_2 rather than NO, and subsequent uptake to aerosol forming 2-MT-OS. OH + isoprene hydroxynitrate also has a small yield of IEPOX (Jacobs et al., 2014). The average diurnal profile of isoprene hydroxynitrates ($C_5H_9NO_4$) in the gas phase measured using the I^--CIMS peaks at around 11:00-12:00 followed by a reduction during the afternoon into the evening/night (SI Figure S6). This is likely to be a result of the relatively low levels of NO during the afternoon, which will reduce isoprene nitrate formation from RO_2 + NO reactions, thus isoprene hydroxynitrates are unlikely to be a significant source of 2-MT-OS in Beijing.

The 2-MT-OS showed a moderate correlation with particulate sulfate (R^2=0.44), and a weak anti-correlation with photochemical age, estimated using the ratio of NO_x/NO_y (R^2=0.23) as shown in Figure 5. All correlations between species are shown in ~~SI Figure S7~~ Figure 5. By taking the product of the concentration of ozone, as a proxy of photochemistry, with the amount of particulate sulfate measured using AMS, $[O_3][pSO_4]$, a much stronger correlation with 2-MT-OS was observed (R^2=0.61) as shown in Figure ~~5~~7. This observation highlights the role of both local photochemistry and particulate sulfate mass in the formation of 2-MT-OS (Figure ~~5~~7). The correlation of $[O_3][pSO_4]$ with 2-MT-OS is likely to be weaker at longer photochemical ages when the ozone concentration is not directly related to the photochemical formation of the OS. Again, this highlights the strong role of local photochemistry in the production of low-NO iSOA (2-MT-OS) in Beijing. Elevated levels of 2-MT-OS were observed at the start and end of the measurement period which were influenced by strong south-westerly winds. There were also elevated isoprene concentrations (up to 2.9 ppb) and high particulate SO_4^{2-} levels. Therefore, these spikes in 2-MT-OS could be a result of either higher 2-MT-OS in regional aerosol transported to the site or a high isoprene emission source to the south west of the site (i.e. producing IEPOX locally) that then reacts with increased regional sulfate pollution. The I-CIMS data shows that the IEPOX/ISOPOOH (Figure S5 and Newland et al., 2020) signal increases during the afternoon as the NO levels drop to below 1 ppb. The low NO levels mean that up to 30 % of the isoprene peroxy radical from OH oxidation can react with HO_2 rather than NO at this site, meaning IEPOX can be formed locally (Newland et al., 2020). There is also likely to be a regional source of IEPOX and 2-MT-OS, suggesting both local and regional anthropogenic influences.

Analysis of the 2-MT-OS isomer distribution using HILIC/ESI-HR-QTOFMS, on a subset of 15 samples, indicates that β-IEPOX is the dominant ambient IEPOX isomer, in line with other recent observations (Cui et al, 2018; Krechmer et al., 2016) see SI Figure S7~~8~~). The MT-OS derived exclusively from δ-IEPOX-OS isomers could not be observed in any of the samples. The 4 IEPOX-OS isomers in SI Figure S7~~8~~ showed similar temporal trends although small changes in the relative proportions were observed. The sum of peak areas from the 2-MT-OS isomers measured by HILIC and the quantified 2-MT-OS (sum of isomers) measured via UPLC/ESI-HR-MS were compared and showed a high degree of correlation (R^2 = 0.84), even though the two methods used different solvents. The agreement indicates that the UPLC/ESI-HR-MS method captures the sum of the isomers and there is no evidence of ion source induced artefacts.

~~3.4~~3.5.2 2-methyl glyceric acid OS (2-MG-OS)

The most common targeted SOA tracer for high-NO isoprene chemistry is 2-methylglyceric acid (2-MG) and its derivatives. As such, this tracer is the result of a direct biogenic-anthropogenic interaction. Two observed SOA tracers related to this chemistry are the OS derivatives of 2-methylglyceric acid (2-MG-OS) and the unresolved C_8 dimers of 2-MG-OS ($C_8H_{14}SO_{10}$) that have been identified previously in chamber-derived iSOA (Surratt et al., 2006; Surratt et al., 2010). 2-MG-OS had an average concentration during the campaign of 21.5 ng m^{-3}, ranging from 0.3 to 180.5 ng m^{-3}, with the time series shown in Figure ~~4~~6b. These values are within the range of 2-MG-OS measured in other urban locations (Nguyen et al., 2014; Rattanavaraha et al., 2016; Hettiyadura et al., 2019). However these concentrations are considerably higher than previously observed at two Chinese regional background sites (Wang et al., 2018; He et al., 2018). At these locations, the ratio of the low-NO to high-NO isoprene OS tracer average concentrations was close to 1.5 (2-MT-OS:2-MG-OS; Beijing = 1.47, Wanqingsha = 1.57). However, in central Beijing, this ratio was considerably lower (2-MT-OS:2-MG-OS = 0.55), reflecting the higher proportion of RO_2 radicals reacting with NO at this location compared to the regional measurements. The ratio of 2-MT-OS:2-MG-OS observed in Beijing is compared to previous studies in Table ~~2~~3 and is considerably lower than measurements taken in a range of isoprene dominated environments (South East US, 2-MT-OS:2-MG-OS = 17, Budisolistiorini et al., 2015.; Amazon, 2-MT-OS:2-MG-OS = 13-118, Glasius et al., (2018).; Atlanta, 2-MT-OS:2-MG-OS = 33, Hettiyadura et al., (2019)) reflecting the strong impact of urban NO emission on iSOA formation. Future work will investigate how to use these ratios to quantify the effect of NO emission on iSOA formation in different regions.

The mean concentration of the 2-MG-OS dimer ($C_8H_{14}SO_{10}$) was 0.57 ng m^{-3}. A strong linear relationship was observed between the 2-MG-OS monomer and dimer concentrations (R^2=0.83) with a dimer:monomer ratio of 0.02. Formation of oligomers from reactions of 2-MG and HMML has been shown to be reduced in chamber experiments under humid conditions (Schwantes et al., 2019; Nestorowicz et al., 2018). The average RH during the afternoon of the campaign was ~40 %, which may account for the relatively low formation of the dimer OS compared to the monomer (see SI Figure 8~~9~~).

The diurnal profile of the 2-MG-OS as shown in ~~SI~~ Figure 8 ~~10~~ was similar to the 2-MT-OS peaking during the early afternoon samples but with an enhanced signal at night. There was also a strong correlation between these two species (R^2 = 0.92) during the campaign. The 2-MG-OS showed a stronger correlation with particulate sulfate (R^2=0.52) than 2-MT-OS (R^2=0.44), and there was also a weak anti-correlation with photochemical age (R^2=0.28). A strong correlation was also observed for 2-MG-OS with [O_3][pSO4] (R^2=0.69), as shown in Figure ~~5~~7, highlighting that formation is dependent on both photochemistry and sulfate aerosol availability.

~~3.4~~3.5.3 Other isoprene-related OSs and NOSs

24 additional OSs species, with molecular formulae consistent with iSOA tracers seen in chamber experiments, were also observed in Beijing as shown in Table ~~1~~2. For C_5 compounds, the most abundant

species were $C_5H_{10}SO_6$ and $C_5H_{10}SO_5$, with mean concentrations of 28.7 ng m^{-3} and 26.5 ng m^{-3}, respectively. The identity of the OS at *m/z* 182 ($C_5H_{10}SO_5$) is currently unknown and the product ion MS provides little additional information other than sulfate-related fragment ions at *m/z* 97 and *m/z* 80. The OS at m/z 198 ($C_5H_{10}SO_6$) was identified as an IEPOX-related OS in chamber experiments by Nestorowicz *et al.* (2018), but at relatively low concentrations compared to the 2-MT-OS (1-4 %). This is very different to the observed ratio is Beijing, where the $C_5H_{10}SO_6$ average concentration was more than double that of 2-MT-OS, as shown in Figure ~~4~~6c. This compound showed a strong correlation with 2-MT-OS (R^2 = 0.77) but it is currently unclear why this compound is the most abundant C_5 species. The molecular weight of this species is 18 Da ($-H_2O$) lower than 2-MT-OS, which may indicate it is a dehydration product enhanced under acidic aerosol conditions. In addition, this species may also be enhanced if it is formed from additional VOC precursors.

Potential low-NO iSOA tracers, seen in chamber experiments, correlated strongly with the 2-MT-OS including unresolved isomers of cyclic hemiacetals [$C_5H_{10}SO_7$ (R^2=0.92)], and lactones [$C_5H_8SO_7$ (R^2=0.83)] (Spolnik et al., 2018). These compounds were similar in concentration to the 2-MT-OS, with the lactones at MW 212 having a mean concentration of 14 ng m^{-3} and the cyclic hemiacetals at MW 214 a mean of 10.6 ng m^{-3}. These compounds were also observed to be the dominant type of isoprene-derived OSs in Atlanta, Georgia, although they had concentrations a factor of ~15 times lower than the observed 2-MT-OS. (Hettiyadura et al., 2019)

Additional small OS compounds, previously identified during high-NO chamber experiments, were also observed in Beijing, including in order of decreasing concentration, glycolic acid sulfate ($C_2H_4SO_6$, mean = 38.4 ng m^{-3}), hydroxyacetone sulfate ($C_3H_6SO_5$, mean = 20.5 ng m^{-3}) and lactic acid sulfate ($C_3H_6SO_6$, mean = 14.5 ng m^{-3}) (Surratt et al., 2007; Surratt et al., 2008). These concentrations are in line with measurements made in other urban locations (Rattanavaraha et al., 2016; Huang et al., 2018; Hettiyadura et al., 2018). While all three C_2-C_3-OS compounds had strong correlations with the other iSOA OS tracers (R^2 = 0.6-0.94), the relative strength of isoprene versus other VOC precursors, such as aromatics, cannot be determined. As such, they cannot be definitively assigned as iSOA tracers, and are therefore included in the potential iSOA portion of Figure ~~6~~9. The sum of the C_2 and C_3 OSs had an average concentration of 73 ng m^{-3}, with a range of 2.0-831 ng m^{-3}.

In addition, 9 NOS species related to isoprene were identified as shown in Table ~~1~~2 (Ng et al., 2008; Rollins et al., 2009). Some of the NOS observed peaked in the daytime and some were enhanced at night. In total they had a mean concentration of 24 ng m^{-3} during the campaign. NOS species are formed via the heterogenous uptake of isoprene nitrates (IN) into the particle phase. Nitrate radicals play a key role in the formation of IN, with nitrate radicals forming from reaction of NO_2 with O_3, both key anthropogenic pollutants. Therefore, emissions of NOx and formation of particulate sulfate will enhance the production of isoprene NOS species.

~~3.5~~3.6 Contribution of Isoprene SOA in Beijing

In order to estimate the total amount of isoprene-derived OSs and NOSs, labelled here as iSOA, 13 species were chosen that could be confidently identified as being predominately from isoprene (2-MT-OS, 2-MG-OS, $C_5H_{10}SO_7$, $C_5H_8SO_7$, $C_5H_{11}NSO_9$, $C_5H_9NSO_{10}$, $C_5H_9N_2SO_{11}$, $C_5H_8N_3SO_{13}$). Although there were a number of other compounds with formula similar to iSOA tracers, their trends compared to previous studies and potential for alternative sources made a confident assignment of VOC precursor difficult. Therefore, the estimated contribution of iSOA to the observed total particulate mass determined here should be taken as a lower limit. Figure ~~6~~9 shows the time series of the iSOA observed in Beijing. The average concentration was 82.5 ng m^{-3} during the campaign, ranging from 718 ng m^{-3} on the 19/05/2017 (11:38 – 14:30) to 1.9 ng m^{-3} on the 02/06/2017 (14:36-17:28). The contribution of iSOA to the OOA factors measured by the AMS was obtained by assuming all OSs and NOSs species fragment in the ion source to lose the sulfate and nitrate groups. Across the whole measurement period, the iSOA tracers represented only a small fraction of the total OOA measured by AMS (0.62% of ∑[OOA1-3]). However, towards the end of the measurement period, this increased up to a maximum of 3 % on the 17/06/2017 (13:32-14:23).

Additional iSOA tracers containing only CHO (Table 3), including 2-methyltetrols, 2-methyglyceric acid and C_5-alkene triols, were measured in separate 24-hour filter samples, with the commonly used derivatization GC-MS method (Claeys et al., 2004; Wang et al., 2005.). The average ratio of the 2-methyltetrols to its corresponding OS (2-MT:2-MT-OS) was 1.4, indicating extensive heterogeneous conversion of isoprene oxidation products within the particles. The observed ratio is slightly larger than those measured in the SE US (~0.37-0.96 as shown in Table ~~2~~3) but much lower than that measured in the Pearl River Delta region (~40,) where the 2-methyltetrols dominated. In contrast, the average ratio of the high-NO iSOA tracer, 2-MG and its corresponding organosulfate (2-MG:2-MG-OS) observed in Beijing was 0.33, indicating more extensive transformation to products from heterogeneous reactions. This ratio may also reflect the more volatile nature of 2-MG compared to 2-MT. Overall, the combined concentrations of these isoprene CHO compounds were generally low (mean 25 ng m^{-3}, max 69 ng m^{-3}) in comparison to the heterogeneous iSOA compounds (i.e., isoprene-derived OSs and NOSs) targeted in this work. In addition, the concentrations of these CHO species may be overestimated based on recent studies demonstrating that thermal decomposition leads to these products being detected by GC-MS and FIGAERO-CIMS methods (D'Ambro et al., 2019), and so the conversion to ~~heterogeneous products~~ products from heterogenous reactions (i.e., OSs and NOSs) may in fact be larger (2MT:2MT-OS = 0.5-0.91 using the overestimates of 160-288 % observed in Cui et al., (2018)).

The study presented here shows for the first time that OS species derived from isoprene oxidation can make a significant contribution to oxidised organic aerosol in Beijing in summer. There is significant anthropogenic control, from both NO_x and sulfate aerosols, on the products and concentrations of iSOA in Beijing. The majority of the OS species showed a strong correlation towards the product of $[O_3][pSO_4]$, highlighting the role of both photochemistry and the availability of particulate sulfate for heterogeneous reactions. When the observed concentrations of all the OS and NOS species measured in this study, including the additional 19 compounds not confidently assigned to iSOA, are combined they contribute

on average 2.2 % to the total OOA (∑[OOA1-3]), increasing to a maximum of 10.5 %, indicating extensive heterogeneous conversion of VOC oxidation products in Beijing in summer.

Author contributions

DB analysed the aerosol samples and quantified iSOA tracers. WD and KP developed the UPLC-MS method. JRH, RD and MS provided the VOC measurements. FS and JL collected the NO, NO_2 and O_3 data. TB, AM, SW, AB, CJP, HC collected and analysed the CIMS data. LW, DH and ES provided the OH and HO_2 data and BO provided the NO_3 measurements. TC, JDS and WD carried out the offline HILIC analysis. DL, ZS and RH provided the GC-MS iSOA data. YS and WX carried out the AMS measurements and PMF analysis. ACL and RH lead the APHH projects. DB, ARR and JFH wrote the manuscript with input and discussion with all co-authors.

Competing interests

The authors declare that they have no conflict of interest.

Acknowledgements

This project was funded by the Natural Environment Research Council, the Newton Fund and Medical Research Council in the UK, and the National Natural Science Foundation of China (NE/N007190/1, NE/N006917/1). We acknowledge the support from Pingqing Fu, Zifa Wang and Jie Li ~~and Yele Sun~~ from IAP for hosting the APHH-Beijing campaign at IAP. We thank Tuan Vu and Bill Bloss from the University of Birmingham, Siyao Yue, Liangfang Wei, Hong Ren, Qiaorong Xie, Wanyu Zhao, Linjie Li, Ping Li, Shengjie Hou, Qingqing Wang from IAP, Kebin He and Xiaoting Cheng from Tsinghua University, and James Allan from the University of Manchester for providing logistic and scientific support for the field campaigns. Daniel Bryant, Freya Squires, William Dixon and Eloise Slater acknowledge NERC SPHERES PhD studentships. Marvin Shaw acknowledges SYFT Technologies for his fellowship grants and scientific support. The Orbitrap-MS was funded by a Natural Environment Research Council strategic capital grant, CC090. Jason Surratt and Tianqu Cui acknowledge support from the United States National Science Foundation (NSF) under Atmospheric and Geospace (AGS) Grant 1703535 as well as thank Avram Gold and Zhenfa Zhang from the University of North Carolina for providing the 2-MT-OS and 2-MG-OS standards.

References

Atkinson, R., Baulch, D. L., Cox, R. A., Crowley, J. N., Hampson, R. F., Hynes, R. G., Jenkin, M. E., Rossi, M. J., Troe, J., and IUPAC Subcommittee: Evaluated kinetic and photochemical data for atmospheric chemistry: Volume II – gas phase reactions of organic species, Atmos. Chem. Phys., 6, 3625-4055, https://doi.org/10.5194/acp-6-3625-2006, 2006.

Bannan, T. J., Booth, A. M., Bacak, A., Muller, J. B., Leather, K. E., Le Breton, M., Jones, B., Young, D., Coe, H., Allan, J., Visser, S., Slowik, J. G., Furger, M., Prévôt, A. S. H., Lee, J., Dunmore, R. E., Hopkins, J. R., Hamilton, J. F., Lewis, A. C., Whalley, L. K., Sharp. T., Stone, D., Heard, D. E., Fleming. Z. L., Leigh, R., Shallcross, D. E., and Percival C. J.: The first UK measurements of nitryl chloride using a chemical ionization mass spectrometer in central London in the summer of 2012, and an investigation of the role of Cl atom oxidation, J. Geophys. Res. Atmos., 120, 5638-5657, https://doi.org/10.1002/2014JD022629, 2015.

Bannan, T. J., Le Breton, M., Priestley, M., Worrall, S. D., Bacak, A., Marsden, N. A., Mehra, A., Hammes, J., Hallquist, M., Alfarra, M. R., Krieger, U, K., Reid, J. P., Jayne, J., Robinson, W., McFiggins, G., Coe, H., Percival, C. J., and Topping, D.: A method for extracting calibrated volatility information from the FIGAERO-HR-ToF-CIMS and its experimental application, Atmos. Meas. Tech., 12, 1429-1439, https://doi.org/10.5194/amt-12-1429-2019, 2019.

Beelen, R., Raaschou-Nielsen, O., Stafoggia, M., Andersen, Z. J., Weinmayr, G., Hoffmann, B., Wolf, K., Samoli, E., Fischer, P., Nieuwenhuijsen, M., Vineis, P., Xun, W. W., Katsouyanni, K., Dimakopoulou, K., Oudin, A., Forsberg, B., Modig, L., Havulinna, A. S., Lanki, T., Turunen, A., Oftedal, B., Nystad, W., Nafstad, P., De Faire, U., Pedersen, N. L., Ostenson, C. G., Fratiglioni, L., Penell, J., Korek, M., Pershagen, G., Eriksen, K. T., Overvad, K., Ellermann, T., Eeftens, M., Peeters, P. H., Meliefste, K., Wang, M., Bueno-de- Mesquita, B., Sugiri, D., Kramer, U., Heinrich, J., de Hoogh, K., Key, T., Peters, A., Hampel, R., Concin, H., Nagel, G., Ineichen, A., Schaffner, E., Probst-Hensch, N., Kunzli, N., Schindler, C., Schikowski, T., Adam, M., Phuleria, H., Vilier, A., Clavel-Chapelon, F., Declercq, C., Grioni, S., Krogh, V., Tsai, M. Y., Ricceri, F., Sacerdote, C., Galassi, C., Migliore, E., Ranzi, A., Cesaroni, G., Badaloni, C., Forastiere, F., Tamayo, I., Amiano, P., Dorronsoro, M., Katsoulis, M., Trichopoulou, A., Brunekreef, B., and Hoek, G.: Effects of long-term exposure to air pollution on natural-cause mortality: an analysis of 22 European cohorts within the multicentre ESCAPE project, Lancet., 383, 785-795, https://doi.org/10.1016/S0140-6736(13)62158-3, 2014.

Brüggemann, M., van Pinxteren, D., Wang, Y., Yu, J. Z. and Herrmann, H.: Quantification of known and unknown terpenoid organosulfates in PM10 using untargeted LC–HRMS/MS: contrasting summertime rural Germany and the North China Plain, Environ. Chem., 16, 333, https://doi.org/10.1071/EN19089, 2019.

Budisulistiorini, S. H., Canagaratna, M. R., Croteau, P. L., Marth, W. J., Baumann, K., Edgerton, E. S., Shaw, S. L., Knipping, E. M., Worsnop, D. R., Jayne, J. T., Gold, A., Surratt, J. D.: Real-time continuous characterization of secondary organic aerosol derived from isoprene epoxydiols in downtown Atlanta, Georgia, using aerodyne aerosol chemical speciation monitor, Environ. Sci. Technol., 47, 5686-5694, https://doi.org/10.1021/es400023n, 2013.

Budisulistiorini, S. H., Baumann, K., Edgerton, E. S., Bairai, S. T., Mueller, S., Shaw, S. L., Knipping, E. M., Gold, A., and Surratt, J. D.: Seasonal characterization of submicron aerosol chemical composition and organic aerosol sources in the southeastern United States: Atlanta, Georgia,and Look Rock, Tennessee, Atmos. Chem. Phys., 16, 5171–5189, https://doi.org/10.5194/acp-16-5171-2016, 2016.

Carlton, A. G., Wiedinmyer, C., Kroll, J. H., and Kroll, J. H.: A review of Secondary organic aerosol (SOA) formation from isoprene, Atmos. Chem. Phys., 9, 4987-5005, https://doi.org/10.5194/acp-9-4987-5005, 2009.

Chan, C. K., Yao, X.: Air pollution in mega cities in China, Atmos. Environ., 42, 1−42, https://doi.org/10.1016/j.atmosenv.2007.09.003, 2008.

Chan, M. N., Surratt, J. D., Claeys, M., Edgerton, E. S., Tanner, R. L., Shaw, S. L., Zheng, M., Knipping, E. M., Eddingsaas, N. C., Wennberg, P. O., and Seinfeld, J. H.: Characterization and quantification of isoprene-derived epoxydiols in ambient aerosol in the Southeastern United States, Environ. Sci. Technol., 44, 4590-4596, https://doi.org/10.1021/es100596b, 2010.

Chen, Q., Farmer, D. K., Rizzo, L. V., Pauliquevis, T., Kuwata, M., Karl, T. G., Guenther, A., Allan, J. D., Coe, H., Andreae, M. O., Pöschl, U., Jimenex, J. L., Artaxo, P., and Martin, S. T.: Submicron particle mass concentrations and sources in the Amazonian wet season (AMAZE-08), Atmos. Chem. Phys., 15, 3687-3701, https://doi.org/10.5194/acp-15-3687-2015, 2015.

Chhabra, P. S., Flagan, R. C., and Seinfeld, J. H.: Elemental analysis of chamber organic aerosol using an aerodyne high-resolution aerosol mass spectrometer, Atmos. Chem. Phys, 10, 4111-4131, ~~https://doi.org/acp-10-4111-2010~~ https://doi.org/10.5194/acp-10-4111-2010, 2010.

Claeys, M., Graham, B., Vas, G., Wang, W., Vermeylen, R., Pashynska, Cafmeyer, J., Guyon, P., Andreae, M. O., Artaxo, P., and Maenhaut, W.: Formation of Secondary Organic Aerosols Through Photooxidation of Isoprene, Science., 303, 1173-1176, https://doi.org/10.1126/science.1092805, 2004.

Clark, C. H., Kacarab, M., Nakao, S., Asa-Awuku, A., Sato, K., and Cocker, D. R.: Temperature Effects on Secondary Organic Aerosol (SOA) from the Dark Ozonolysis and Photo-Oxidation of Isoprene, Environ. Sci. Technol., 50, 5564-5571, https://doi.org/10.1021/acs.est.5b05524, 2016.

Cui, T., Zeng, Z., dos Santos, E. O., Zhang, Z., Chen, Y., Zhang, Y., Rose, C. A., Budisulisyiorini, S. H., Collins, L. B., Bodnar, W. M., de Souza, R. A. F., Martin, S. T., Machado, C. M. D., Turpin, B. J., Gold, A., Ault, A. P., and Surratt, J. D: Development of hydrophilic interaction liquid chromatography (HILIC) method for the chemical characterization of water-soluble isoprene epoxydiol (IEPOX)-derived secondary organic aerosol, Environ. Sci. Processes Impacts, 20, 1524-1536, https://doi.org/10.1039/c8em00308d, 2018.

D'Ambro, E. L., Schobesberger, S., Gaston, C. J., Lopez-Hilfiker, F. D., Lee, B. H., Liu, J., Zelenyuk, A., Bell, D., Cappa, C. D., Helgestad, T., Li, Z., Guenther, A., Wang, J., Wise, M., Caylor, R., Surratt, J. D., Riedel, T., Hyttinen, N., Salo, V. -T., Hasan, G., Kurtén, T., Shilling, J. E., and Thornton, J. A.: Chamber-based insights into the factors controlling IEPOX SOA yield, composition, and volatility., Atmos. Chem. Phys. Discuss., 19, 11253-11265, https://doi.org/10.5194/acp-2019-271, 2019.

Ding, X., He, Q. -F., Shen, R. -Q., Yu, Q. -Q., and Wang, X. -M.: Spatial distributions of secondary organic aerosols from isoprene, monoterpenes, β-caryophyllene, and aromatics over China during summer, J. Geophys. Res. Atmos., 119, 11877-11891, http://doi.org/10.1002/2014JD021748, 2014.

Dockery, D. W., Pope, C. A., Xu, X. P., Spengler, J. D., Ware, J. H., Fay, M. E., Ferris, B. G., Speizer, F. E.: An Association between Air- Pollution and Mortality in 6 United-States Cities, N. Engl. J. Med., 329, 1753−1759, https://doi.org/10.1056/NEJM199312093292401, 1993.

Dommen, J., Metzger, A., Duplissy, J., Kalberer, M., Alfarra, M. R., Gascho, A., Weingartner, E., Prevot, A. S. H., Vergeggen and B., Baltensperger.: Laboratory observation of oligomers in the aerosol from isoprene/NO_X photooxidation, Geophys. Res. Lett., 33, L13805, https://doi.org/10.1029/2006GL026523, 2016.

Edney, E. O., Kleindienst, T. E., Jaoui, M., Lewandowksi, M., Offenberg, J. H., Wang, W., and Claeys, M.: Formation of 2-methyl tetrols and 2-methylglyceric acid in secondary organic aerosol from laboratory irradiated isoprene/NO_X/SO_2/air mixtures and their detection in ambient $PM_{2.5}$ samples collected in the eastern United States, Atmospheric. Environ., 39, 5281-5289, ~~https://doi.org/10.1016/j/atmosenv.2005.05.031~~, https://doi.org/10.1016/j.atmosenv.2005.05.031, 2005.

Fu, P., Kawamura, K., Kanaya, Y., and Wang, Z.: Contributions of biogenic volatile organic compounds to the formation of secondary organic aerosols over Mt. Tai, Central East China, Atmos. Environ., 44, 4817-4826., https://doi.org/10.1016/j.atmosenv.2010.08.040, 2010.

Gaston, C. J., Riedel, T. P., Zhang, Z., Gold, A., Surratt, J. D., and Thornton, J. A.: Reactive uptake of an isoprene-derived epoxydiol to submicron aerosol particles, Environ. Sci. Technol., 48, 11178-11186, https://doi.org/10.1021/es5034266, 2014.

Glasius, M., Bering, M. S., Yee, L. D., De Sá, S. S., Isaacman-VanWertz, G., Wernis, R. A., Barbosa, H. M. J., Alexander, M. L., Palm, B. B., Hu, W., Campuzano-Jost, P., Day, D. A., Jimenez, J. L., Shrivastava, M., Martin, S. T., and Goldstein, A. H.: Organosulfates in aerosols downwind of an urban region in central Amazon, Environ. Sci.: Process. Impact., 20, 1546-1558., https://doi.org/10.1039/c8em00413g, 2018.

Hamilton, J. F., Lewis, A. C., Carey, T. J., and Wenger, J. C.: Characterization of Polar Compounds and Oligomers in Secondary Organic Aerosol Using Liquid Chromatography Coupled to Mass Spectrometry, Anal. Chem., 80, 474-480, https://doi.org/10.1021/ac701852t, 2008.

He, Q. -F., Ding, X., Fu, X. -X., Zhang, Y. -Q., Wang, J. -Q., Liu, Y. -X., Tang, M. -J., Wang, X. -M., and Rudich, Y.: Secondary Organic Aerosol Formation From Isoprene Epoxides in the Pearl River

Delta, South China: IEPOX- and HMML- Derived Tracers, J. Geophys. Res. Atmos., 123, 6999-7012, https://doi.org/10.1029/2017JD028242, 2018.

Hettiyadura, A. P. S., Al-Naiema, I. M., Hughes, D. D., Fang, T., and Stone, E. A.: Organosulfates in Atlanta, Georgia: anthropogenic influences on biogenic secondary organic aerosol formation, Atmos. Chem. Phys., 19, 3191-3206, https://doi.org/10.5194/acp-19-3191-2019, 2019.

Hettiyadura, A. P. S., Xu, L., Jayarathne, T., Skog, K., Guo, H., Weber, R. J., Nenes, A., Keutsch, F. N., Ng, N. L., and Stone, E. A.: Source apportionments of organic in Centreville, AL using organosulaftes in organic tracer-based positive matrix factorization, Atm. Environ., 186, 74-88, https://doi.org/10.1016/j.atmosenv.2018.05.007, 2018.

Hopkins, J. R., Jones, C. E., and Lewis, A. C.: A dual channel gas chromatograph for atmospheric anlysis of volatile organic compounds including oxygenated and monoterpene compounds, J. Environ. Monit., 13, 2268-2276, ~~https://doi.org/10.1039/clem10050e,~~ https://doi.org/10.1039/C1EM10050E, 2011.

Hu, J., Huang, L., Chen, M., Liao, H., Zhang, H., Wang, S., Zhang, Q., and Ying, Q.: Premature Mortality Attributable to Particulate Matter in China: Source Contributions and Responses to Reductions, Environ. Sci. Technol., 51, 9950-9959, https://doi.org/10.1021/acs.est.7b03193, 2017a.

Hu, J., Li, Xun., Huang, L., Ying, Q., Zhang, Q., Zhao, B., Wang, S., and Zhang, H.: Ensemble prediction of air quality using the WRF/CMAQ model system for health effect studies in China, Atmos. Chem. Phys., 17, 13103-13118, https://doi.org/10.5194/acp-17-13103-2017, 2017b.

Hu, J., Wang, Y., Ying, Q., Zhang, H.: Spatial and temporal variability of PM2.5 and PM10 over the North China Plain and the Yangtze River Delta, China, Atmos. Environ., 95, 598−609, https://doi.org/10.1016/j.atmosenv.2014.07.019, 2014.

Hu, W. W., Campuzano-Jost, P., Palm, B. B., Day, D. A., Ortega, A. M., Hayes, P. L., Krechmer, J. E., Chen, Q., Kuwata, M., Liu, Y. J., De Sá, S. S., McKinney, K., Martin, S. T., Hu, M., Budisulistiorini, S. H., Riva, M., Surratt, J. D., St. Clair, J. M., Isaacman-Van Wertz, G., Yee, L. D., Goldstein, A. H., Carbon, S., Brito, J., Artaxo, P., De Gouw, J. A., Koss, A., Wisthaler, A., Mikoviny, T., Karl, T., Kaser, L., Jud, W., Hansel, A., Doucherty, K, S., Alexander, M. L., Robinson, N. H., Coe, H., Allan, J. D., Canagaratna, M. R., Paulot, F., and Jimenez, J. L.: Characterization of a real-time tracer for isoprene epoxydiols-derived secondary organic aerosol (IEPOX-SOA) from aerosol mass spectrometer measurements, Atmos. Chem. Phys., 15, 11807-11833, https://doi.org/10.5194/acp-15-11807-2015, 2015.

Hu, W., Hu, M., Hu, W., Jimenez, J. L., Yuan, B., Chen, W., Wang, M., Wu, Y., Chen, C., Wang, Z., Peng, J., Zeng, L., and Shao, M.: Chemical Composition, sources, and aging process of submicron aerosols in Beijing: Contrast between summer and winter, J. Geophys. Res. Atmos., 121, 1955-1977, https://doi.org/10.1002/2015JD024020, 2016.

Huang, R. -J., Cao, J., Chen, Y., Yang, L., Shen, J., You, Q., Wang, K., Lin, C., Xu, W., Gao, B., Li, Y., Chen, Q., Hoffmann, T., O'Dowd, C. D., Bilde, M., and Glasius.: Organosulfates in atmospheric aerosol: Synthesis and quantitative analysis of $PM_{2.5}$ from Xi'an, northwestern China, Atmos. Meas. Tech., 11, 3447-3456, https://doi.org/10.5194/amt-11-3447-2018, 2018.

Jacobs, M. I., Burke, W. J., and Elrod, M. J.: Kinetics of the reactions of isoprene-derived hydroxynitrates: gas phase epoxide formation and solution phase hydrolysis, Atmos. Chem. Phys., 14, 8933-8946, https://doi.org/10.5194/acp-14-8933-2014, 2014.

Jerrett, M., Burnett, R. T., Pope, C. A., Ito, K., Thurston, G., Krewski, D., Shi, Y. L., Calle, E., Thun, M.: Long-Term Ozone Exposure and Mortality, N. Engl. J. Med., 2009, 360, 1085−1095, https://doi.org/10.1056/NEJMoa0803894, 2009.

Kleindienst, T. E., Edney, O. E., Lewandowski, M., Offenberg, and J. H., Jaoui, M.: Secondary organic carbon and aerosol yields from the irradiations of isoprene and α-pinene in the presence of NOx and SO2, Environ. Sci. Technol., 40, 3807-3812, https://doi.org/10.1021/es052446r, 2016.

Kleindienst, T. E., Jaoui, M., Lewandowski, M., Offenberg, J. H., Lewis, C. W., Bhave, P. V., and Edney, E. O.: Estimates of the contributions of biogenic and anthropogenic hydrocarbons to secondary organic aerosol at a southeastern US location, Atmos. Environ., 41, 8288-8300, http://doi.org/10.1016/j.atmosenv.2007.06.045, 2007.

Krechmer, J. E., Coggon, M. M., Massoli, P., Nguyen, T. B., Crounse, J. D., Hu, W., Day, D. A., Tyndall, G. S., Henze, D. K., Rivera-Rios, J. C., Nowak, J. B., Kimmel, J. R., Mauldin, R. L., Stark, H., Jayne, J. T., Sipilä, M., Junninen, H., St.Clair, J. M., Zhang, X., Feiner, P. A., Zhang, L., Miller, D. O., Brune, W. H., Keutsch, F. N., Wennberg, P. O., Seinfeld, J. H., Worsnop, D. R., Jimenez, J. L., and Canagaratna, M. R.: Formation of Low Volatility Organic Compounds and Secondary Organic Aerosol from Isoprene Hydroxyhydroperoxide Low-NO Oxidation, Environ. Sci. Technol., 49, 10330-10339, https://doi.org/10.1021/acs.est.5b02031, 2015.

Krechmer, J. E., Groessl, M., Zhang, X., Junninen, H., Massoli, P., Lambe, A. T., Kimmel, J. R., Cubison, M. J., Graf, S., Lin, Y. -H., Budisulistiorini, S. H., Zhang, H., Surratt, J. D., Knochenmuss, R., Jayne, J. T., Worsnop, D. R., Jimenez, J. -L., and Canagaratna, M. R.: Ion mobility spectrometry-mass spectrometry (IMS-MS) for on- and offline analysis of atmospheric gas and aerosol species, Atmos. Meas. Tech., 9, 3245-3262, https://doi.org/10.5194/amt-9-3245-2016, 2016.

Kroll, J. H., Ng, N. L., Murphy, S. M., Flagan, R. C., and Seinfeld, J. H.: Secondary organic aerosol formation from isoprene photooxidation, Environ. Sci. Technol., 40, 1869-1877, https://doi.org/10.1021/es0524301, 2006.

Laurent, O., Hu, J. L., Li, L. F., Cockburn, M., Escobedo, L., Kleeman, M. J., Wu, J.: Sources and contents of air pollution affecting term low birth weight in Los Angeles County, California, 2001−2008, Environ. Res., 134, 488−495, https://doi.org/10.1016/j.envres.2014.05.003, 2014.

Le Breton, M., Bacak, A., Muller, J. B. A., Bannan, T. J., Kennedy, O., Ouyang, B., Xiao, P., Bauguitte, S. J. -B., Shallcross, D. E., Jones, R. L., Daniels, M. J. S., Ball, S. M., and Percival, C. J.: The first airbourne comparison of N_2O_5 measurements over the UK using a CIMS and BBCEAS during the RONOCO campaign, Anal. Methods., 6, 9731-9743, https://doi.org/10.1039/C4AY02273D, 2014.

Le Breton, M., Wang, Y., Hallquist, A. M., Kant Pathak, R., Zheng, J., Yang, Y., Shang, D., Glasius, M., Bannan, T. J., Liu, Q., Chank, C. K., Percival, C. J., Zhu, W., Lou, S., Topping, D., Wang, Y., Yu, J., Lu, K., Guo, S., Hu, M., and Hallquist, M.: Online gas- and particle-phase measurements of organosulfates, orgnanosulfonates and nitrooxy organosulaftes in Beijing utilizing a FIGAERO ToF-CIMS, 18, 10355-10371, https://doi.org/10.5194/acp-18-10355-2018, 2018.

Lee, B. H., Lopez-Hilfiker, F. D., Mohr, C., Kurtén, T., Worsnop, D. R., and Thornton, J. A.: An iodide-adduct high-resolution time-of-flight chemical-ionization mass spectrometer: Application to atmospheric inorganic and organic compounds, Environ. Sci. Technol., 48, 6309-6317, https://doi.org/10.1021/es500362a, 2014.

Lelieveld, J., Evans, J. S., Fnais, M., Giannadaki, D., Pozzer, A.: The contribution of outdoor air pollution sources to premature mortality on a global scale, Nature., 525, 367-371, https://doi.org/10.1038/nature15371, 2015.

Li, J., Wang, G., Wu, C., Cao, C., Ren, Y., Wang, J., Li, J., Cao, J., Zeng, L., and Zhu, T.: Characterization of isoprene-derived secondary organic aerosols at a rural site in North China Plain with implications for anthropogenic pollution effects, Sci. Rep., 8, 535, https://doi.org/10.1038/s41598-017-18983-7, 2018.

Lin, Y. -H., Zhang, H., Pye, H. O. T., Zhang, Z., Marth, W. J., Park, S., Arashiro, M., Cui, T., Budisulistiorini, S. H., Sexton, K. G., Vizuete, W., Xie, Y., Luecken, D. J., Piletic, I. R., Edney, E. O., Bartolotti, L. J., Gold, A., and Surratt, J. D.: Epoxide as a precursor to secondary organic aerosol formation from isoprene photooxidation in the presence of nitrogen oxides, PNAS, 110, 6718-6723, https://doi.org/10.1073/pnas.1221150110, 2013.

Lin, Y. -H., Zhang, Z., Docherty, K. S., Zhang, H., Budisulistiorini, S. H., Rubitschun, C. L., Shaw, S. L., Knipping, E. M., Edgerton, E. S., Kleindienst, T. E., Gold, A., and Surratt, J. D.: Isoprene epoxydiols as precursors to secondary organic aerosol formation: Acid-catalyzed reactive uptake studies with authentic standards, Environ. Sci. Technol., 46, 250-258, https://doi.org/10.1021/es202554c, 2012.

Lopez-Hilfiker, F. D., Mohr, C., Ehn, M., Rubach, F., Kleist, E., Wildt, J., Mentel, Th. F., Lutz, A., Hallquist, M., Worsnop, D., and Thornton, J. A.: A novel method for online analysis of gas and particle composition: description and evaluation of a Filter Inlet for Gases and Aerosols (FIGAERO), Atmos. Meas. Tech., 7, 983-1001,https://doi.org/10.5194/amt-7-983-2014, 2014.

Lu, K. D., Rohrer, F., Holland, F., Fuchs, H., Brauers, T., Oebel, A., Dlugi, R., Hu, M., Li, X., Lou, S. R., Shao, M., Zhu, T., Wahner, A., Zhang, Y. H., and Hofzumahaus, A.: Nighttime observation and chemistry of HOx in the Pearl River Delta and Beijing in summer 2006, Atmos. Chem. Phys., 14, 4979–4999, https://doi.org/10.5194/acp-14-4979-2014, 2014.

Nestorowicz, K., Jaoui, M., Jan Rudzinski, K., Lewandowski, M., Kleindienst, T. E., Spólnik, G., Danikiewicz, W., and Szmigielski, R.: Chemical composition of isoprene SOA under acidic and non-acidic conditions: Effect of relative humidity, Atmos. Chem. Phys., 18, 18101-18121, https://doi.org/10.5194/acp-18-18101-2018, 2018.

Newland, M. J., Bryant, D. J., Dunmore, R. E., Bannan, T. J., Acton, W. J. F., Langford, B., Hopkins, J. R., Squires, F. A., Dixon, W., Drysdale, W. S., Ivatt, P. D., Evans, M. J., Edwards, P. M., Whalley, L. K., Heard, D. E., Slater, E. J., Woodward-Massey, R., Ye, C., Mehra, A., Worrall, S. D., Bacak, A., Coe, H., Percival, C. J., Hewitt, C. N., Lee, J. D., Cui, T., Surratt, J. D., Wang, X., Lewis, A. C., Rickard, A. R., and Hamilton, J. F.: Rainforest-like Atmospheric Chemistry in a Polluted Megacity, Atmos. Chem. Phys. Discuss., https://doi.org/10.5194/acp-2020-35, in review, 2020.

Ng, N. L., Kroll, J. H., Keywood, M. D., Bahreini, R., Varutbangkul, V., Flagan, R. C., Seinfeld, J. H., Lee, A., and Goldstein, A. H.: Contribution of first-versus second-generation products to secondary organic aerosols formed in the oxidation of biogenic hydrocarbons, Environ. Sci. Technol., 40, 2283-2297, https://doi.org/10.1021/es052269u, 2006.

Ng, N. L., Kwan, A. J., Surratt, J. D., Chan, A. W. H., Chhabra, P. S., Sorooshian, A., Pye, H. O. T., Crounse, J. D., Wennberg, P. O., Flagan, R. C., Seinfeld, J. H.: Secondary organic aerosol (SOA) formation from reaction of isoprene with nitrate radicals (NO_3), Atmos. Chem. Phys., 8, 4117–4140, https://doi.org/10.5194/acp-8-4117-2008, 2008.

Nguyen, Q. T., Christensen, M. K., Cozzi, F., Zare, A., Hansen, A. M. K., Kristensen, K., Tulinius, T. E., Madsen, H. H., Christensen, J. H., Brandt, J., Massling, A., Nøjgaard, J. K., and Glasius, M.: Understanding the anthropogenic influence on formation of biogenic secondary organic aerosols in Denmark via analysis of organosulfates and related oxidation products, Atmos. Chem. Phys., 14, 8961-8981, https://doi.org/10.5194/acp-14-8961-2014, 2014.

Nguyen, T. B., Bates, K. H., Crounse, J. D., Schwantes, R. H., Zhang, X., Kjaergaard, H. G., Surratt, J. D., Lin, P., Laskin, A., Seinfeld, J. H., and Wennberg, P. O.: Mechanism of the hydroxyl radical oxidation of methacryloyl peroxynitrate (MPAN) and its pathway toward secondary organic aerosol formation in the atmosphere, Phys. Chem. Chem. Phys., 17, 17914-17926, https://doi.org/10.1039/c5cp02001h, 2015.

Nguyen, T. B., Coggon, M. M., Bates, K. H., Zhang, X., Schwantes, R. H., Schilling, K. A., Loza, C. L., Flagan, R. C., Wennberg, P. O., and Seinfeld, J. H.: Organic aerosol formation from the reactive uptake of isoprene epoxydiols (IEPOX) onto non-acidified inorganic seeds, Atmos. Chem. Phys., 14, 3497-3510, https://doi.org/10.5194/acp-14-3497-2014, 2014.

Nguyen, T. B., Roach, P. J., Laskin, J., Laskin, A., and Nizkorodov.: Effect of humidity on the composition of isoprene photooxidation secondary organic aerosol, Atmos. Chem. Phys., 11, 6931-6944, https://doi.org/10.5194/acp-11-6931-2011, 2011.

Ostro, B., Hu, J., Goldberg, D., Reynolds, P., Hertz, A., Bernstein, L., Kleeman, M. J.: Associations of Mortality with LongTerm Exposures to Fine and Ultrafine Particles, Species and Sources: Results from the California Teachers Study Cohort, Environ. Health Perspect., 123, 549−556, https://doi.org/10.1289/ehp.1408565, 2015.

Pandis, S. N., Paulson, S. E., Seinfeld, J. H., and Flagan, R. C.: Aerosol formation in the photooxidation of isoprene and β-pinene, Atmospheric. Environ. Part A. General Topics., 25, 997-1008, https://doi.org/10.1016/0960-1686(91)90141-S, 1991.

Paulot, F., Crounse, J. D., Kjaergaard, H. G., Kürten, A., Clair, J. M. S., Seinfeld, J. H., and Wennberg, P. O.: Unexpected epoxide formation in the gas-phase photooxidation of isoprene, Science, 325, 730-733, https://doi.org/10.1126/science.1172910, 2009.

Pope, C. A., Dockery, D. W.: Health effects of fine particulate air pollution: Lines that connect, J. Air Waste Manage. Assoc., 56, 709−742, https://doi.org/10.1080/10473289.2006.10464485, 2006.

Pope, C. A.: Review: Epidemiological basis for particulate air pollution health standards, Aerosol Sci. Technol., 32, 4−14, https://doi.org/10.1080/027868200303885, 2000.

Priestley, M., Le Breton, M., Bannan, T. J., Leather, K. E., Bacak, A., Reyes-Villegas, E., De Vocht., F., Shallcross, B. M. A., Brazier, T., Khan, M. A., Allan, J., Shallcross, D., E., Coe, H., Percival, C. J.: Observations of isocyanate, amide, nitrate and nitro compounds from an anthropogenic biomass burning event using a ToF-CIMS, Journal of Geophysical Research: Atmospheres, 123, 7687-7704, https://doi.org/10.1002/2017JD027316, 2018.

Rattanavaraha, W., Chu, K., Budisulistiorini, S. H., Riva, M., Lin, Y. -H., Edgerton, E. S., Baumann, K., Shaw, S. L., Guo, H., King, L., Weber, R. J., Neff, M. E., Stone, E. A., Offenberg, J. H., Zhang, Z., Gold, A., and Surratt, J. D.: Assessing the impact of anthropogenic pollution on isoprene-derived secondary organic aerosol formation in $PM_{2.5}$ collected from Birmingham, Alabama, ground site during the 2013 Southern Oxidant and Aerosol Study, Atmos. Chem. Phys., 16, 4897-4914, https://doi.org/10.5194/acp-16-4897-2016, 2016.

Rattanavaraha, W., Canagaratna, M. R., Budisulistiorini, S. H., Croteau, P. L., Baumann, K., Canonaco, F., Prevot, A. S. H., Edgerton, E. S., Zhang, Z., Jayne, J. T., Worsnop, D. R., Gold, A., Shaw, S. L., and Surratt, J. D, Atmos. Environ., 167, 389-402, https://doi.org/10.1016/j.atmosenv.2017.07.055, 2017.

Riva, M., Budisulistiorini, H., Zhang, Z., Gold, A., Surratt, J. D.:Chemical characterization of secondary organic constituents from isoprene ozonolysis in the presence of acidic aerosol, Atmos. Environ., 130, 5-13, https://doi.org/10.1016/j.atmosenv.2015.06.027, 2016a.

Riva, M., Budisulistiorini, S. H., Chen, Y., Zhang, Z., D'Ambro, E. L., Zhang, X., Gold, A., Turpin, B. J., Thornton, J. A., canagaratna, M. R., and Surratt, J. D.: Chemical Characterization of Secondary Organic Aerosol from Oxidation of Isoprene Hydroxyhydroperoxides, Environ. Sci. Technol., 50, 9889-9899, ~~https://doi.org/10.1021/acs.est.5b05524,~~ https://doi.org/10.1021/acs.est.6b02511, 2016b.

Riva, M., Chen, Y., Zhang, Y., Lei, Z., Olson, N. E., Boyer, H. C., Narayan, S., Yee, L. D., Green, H. S., Cui, T., Zhang, Z., Baumann, K., Fort, M., Edgerton, E., Budisulistiorini, S. H., Rose, C. A., Riberiro, I. O., Oliveira, R. L., dos Santa, E. O., Machado, C. M. D., Szopa, S., Zhao, Y., Alves, E. G., de Sá, S. S., Hu, W., Knipping, E. M., Shaw, S. L., Duvoisin, S. Jr., de Souza, R. A. F., Palm, B. B., Jimenez, J. -L., Glasius, M., Goldstein, A. H., Pye, H. O. T., Gold, A., Turpin, B. J., Vizuete, W., Martin, S. T., Thornton, J. A., Dutcher, C. S., Ault, A. P., and Surratt, J. D.: Increasing Isoprene Epoxydiol-to-inorganic Sulfate Aerosol ratio results in Extensive Conversion of Inorganic Sulfate to Organosulfur Forms: Implications for Aerosol Physicochemical Properties, Environ. Sci. Technol., 53, 8682-8694, https://doi.org/10.1021/acs.est.9b01019, 2019.

Riva, M., Rantala, P., Krechmer, E. J., Peräkylä, O., Zhang, Y., Heikkinene, l., Garmash, O., Yan, C., Kulmala, M., Worsnop, D., and Ehn, M.: Evaluating the performance of five different chemical ionization techniques for detecting gaseous oxygenated organic species, Atmos. Meas. Tech., 12, 2403-2421, https://doi.org/10.5194/amt-12-2403-2019, 2019.

Robinson, N. H., Hamilton, J. F., Allan, J. D., Langford, B., Oram, D. E., Chen, Q., Docherty, K., Farmer, D. K., Jimenez, J. L., Ward, M. W., Hewitt, C. N., Barley, M. H., Jenkin, M. E., Rickard, A. R., Martin, S. T., McFiggans, G., and Coe, H.: Evidence for a significant proportion of secondary organic aerosol from isoprene above a maritime tropical forest, Atmos. Chem. Phys., 11, 1039-1050, https://doi.org/10.5194/acp-11-1039-2011, 2011.

Rollins, A. W., Kiendler-Scharr, A., Fry, J. L., Brauers, T., Brown, S. S., Dorn, H. -P., Dubé, W. P., Fuchs, H., Mensah, A., Mentel, T. F., Rohrer, F., Tillman, R., Wegener, R., Woolridge, P. J., and Cohen, R. C: Isoprene oxidation by nitrate radical: alkyl nitrate and secondary organic aerosol yields, Atmos. Chem. Phys., 9, 6685-6703, https://doi.org/10.5194/acp-9-6685-2009, 2009.

Schwantes, R. H., Charan, S. M., Bates, K. H., Huang, Y., Nguyen, T. B., Mai, H., Kong, W., Flagan, R. C., and Seinfeld, J. H.: Low-volatility compounds contribute significantly to isoprene secondary organic aerosol (SOA) under high-NO_X conditions, Atmos. Chem. Phys., 19, 7255-7278, https://doi.org/10.5194/acp-19-7255-2019, 2019.

Shi, Z., Vu, T., Kotthaus, S., Grimmond, S., Harrison, R. M., Yue, S., Zhu, T., Lee, J., Han, Y., Demuzere, M., Dunmore, R. E., Ren, L., Liu, D., Wang, Y., Wild, O., Allan, J., Barlow, J., Beddows, D., Bloss, W. J., Carruthers, D., Carslaw, D. C., Chatzidiakou, L., Crilley, L., Coe, H., Dai, T., Doherty, R., Duan, F., Fu, P., Ge, B., Ge, M., Guan, D., Hamilton, J. F., He, K., Heal, M., Heard, D., Hewitt, C. N., Hu, M., Ji, D., Jiang, X., Jones, R., Kalberer, M., Kelly, F. J., Kramer, L., Langford, B., Lin, C., Lewis, A. C., Li, J., Li, W., Liu, H., Loh, M., Lu, K., Mann, G., McFiggans, G., Miller, M., Mills, G., Monk, P., Nemitz, E., O'Connor, F., Ouyang, B., Palmer, P. I., Percival, C., Popoola, O., Reeves, C., Rickard, A. R., Shao, L., Shi, G., Spracklen, D., Stevenson, D., Sun, Y., Sun, Z., Tao, S., Tong, S., Wang, Q., Wang, W., Wang, X., Wang, Z., Whalley, L., Wu, X., Wu, Z., Xie, P., Yang, F., Zhang, Q., Zhang, Y., Zhang, Y., and Zheng, M.: Introduction to Special Issue – In-depth study of air pollution sources and processes within Beijing and its surrounding region(APHH-Beijing), Atmos. Chem. Phys., 19, 7519-7546, https://doi.org/10.5194/acp-19-7519-2019, 2019.

Spolnik, G., Wach, P., Rudzinski, K. J., Skotak, K., Danikiewicz, W., and Szmigielski, R.: Improved UHPLC-MS/MS Methods for Analysis of Isoprene-Derived Organosulfates, Anal. Chem., 90, 3416-3423, https://doi.org/10.1021/acs.analchem.7b05060, 2018.

Sun, Y., Xu, W., Zhang, Q., Jiang, Q., Canonaco, F., Prévôt, A. S. H., Fu, P., Li, J., Jayne, J., Worsnop, D. R., and Wang, Z.: Source apportionment of organic aerosol from 2-year highly time resolved measurements by an aerosol chemical speciation monitor in Beijing, China, Atmos. Chem. Phys., 18, 8469-8489, https://doi.org/10.5194/acp-18-8469-2018, 2018.

Surratt, J. D., Chan, A. W. H., Eddingsaas, N. C., Chan, M., Loza, C. L., Kwan, A. J., Hersey, S. P., Flagan, R. C., Wennberg, P. O., and Seinfeld. J. H.: Reactive intermediates revealed in secondary organic aerosol formation from isoprene, PNAS., 107, 6640-6645, https://doi.org/10.1073/pnas.0911114107, 2010.

Surratt, J. D., Gómez-González, Y., Chan, A. W. H., Vermeylen, R., Shahgholi, M., Kleindienst, T. E., Edney, E. O., Offenberg, J. H., Lewandowski, M., Jaoui, M., Maenhaut, W., Claeys, M., Flagan, R. C., and Seinfeld, J. H.: Organosulfate formation in biogenic secondary organic aerosol, J. Phys. Chem. A., 112, 8345-8378, https://doi.org/10.1021/jp802310p, 2008.

Surratt, J. D., Kroll, J. H., Kleindienst, T. E., Edney, E. O., Claeys, M., Sorooshian, A., Ng, N. L., Offenberg, J. H., Lewandowski, M., Jaoui, M., Flagan, R. C., and Seinfeld, J. H.: Evidence for organosulfates in secondary organic aerosol, Environ. Sci. Technol., 41, 517-527, https://doi.org/10.1021/es062081q, 2007a.

Surratt, J. D., Lewandowski, M., Offenberg, J. H., Jaoui, M., Kleindienst, T. E., Edney, E. O., and Seinfeld, J. H.: Effect of acidity on secondary organic aerosol formation from isoprene, Environ. Sci. Technol., 41, 5363-5369, https://doi.org/10.1021/es0704176, 2007b.

Surratt, J. D., Murphy, S. M., Kroll, J. H., Ng, N. L., Hildebrandt, L., Sorooshian, A., Szmigielski, R., Vermeylen, R., Maenhaut, W., Claeys, M., Flagan, R. C., and Seinfeld, J. H.: Chemical composition of

secondary organic aerosol formed from the photooxidation of isoprene, J. Phys. Chem. A., 110, 9665-9690, https://doi.org/10.1021/jp061734m, 2006.

Wang, Q., He, X., Huang, H. X. H., Griffith, S. M., Feng, Y., Zhang, T., Zhang, Q., Wu, D., and Yu, J. Z.: impact of Secondary Organic Aerosol Tracers on Tracer-Based Source Apportionment of Organic Carbon and $PM_{2.5}$: A Case Study in the Pearl River Delta, China, ACS Earth Space Chem., 1, 562-571, https://doi.org/10.1021/acsearthspacechem.7b00088, 2017.

Wang, W., Kourtchev, I., Graham, B., Cafmeyer, J., Maenhaut, W., and Claeys, M.: Characterization of oxygenated derivatives of isoprene related to 2-methyltetrols in Amazonian aerosols using trimethylsilylation and gas chromatography/ion trap mass spectrometry, Rapid Commun. Mass Spectrom., 19, 1343-1351, https://doi.org/10.1002/rcm.1940, 2005.

Wang, X., Hayeck, N., Brüggemann, M., Yao, L., Chen, H., Zhang, C., Emmelin, C., Chen, J., George, C. and Wang, L.: Chemical Characteristics of Organic Aerosols in Shanghai: A Study by Ultrahigh-Performance Liquid Chromatography Coupled With Orbitrap Mass Spectrometry, J. Geophys. Res. Atmos., 122, 11,703-11,722, https://doi.org/10.1002/2017JD026930, 2017.

Wang, Y., Zhuang, G., Tang, A., Yuan, H., Sun, Y., Chen, S., and Zheng, A.: The ion chemistry and the source of $PM_{2.5}$ aerosol in Beijing, Atmos. Environ., 39, 3771-3784, https://doi.org/10.1016/j.atmosenv.2005.03.013, 2005.

Wang, Y., Hu, M., Guo, S., Wang, Y., Zheng, J., Yang, Y., Zhu, W., Tang, R., Li, X., Liu, Y., Le Breton, M., Du, Z., Shang, D., Wu, Y., Wu, Z., Song, Y., Lou, S., Hallquist, M., and Yu, J.: The secondary formation of organosulfates under interactions between biogenic emissions and anthropogenic pollutants in summer in Beijing, Atmos. Chem. Phys., 18, 10693-10713, https://doi.org/10.5194/acp-18-10693-2018, 2018.

Wennberg, P. O., Bates, K. H., Crounse, J. D., Dodson, L. G., McVay, R. C., Mertens, L. A., Nguyen, T. B., Praske, E., Schwantes, R. H., Smarte, M. D., St Clair, J. M., Teng, A. P., Zhang, X., and Seinfeld, J. H.: Gas-Phase Reactions of Isoprene and Its Major Oxidation Products, Chem. Rev., 118, 3337-3390, http://doi.org/10.1021/acs.chemrev.7b00439, 2018.

Whalley, L. K., Furneaux, K. L., Goddard, A., Lee, J. D., Mahajan, A., Oetjen, H., Read, K. A., Kaaden, N., Carpenter, L. J., Lewis, A. C., Plane, J. M. C., Saltzman, E. S., Wiedensohler, A., and Heard, D. E.: The chemistry of OH and HO2 radicals in the boundary layer over the tropical Atlantic Ocean, Atmos. Chem. Phys., 10, 1555–1576, https://doi.org/10.5194/acp-10-1555-2010, 2010.

Whalley, L. K., Stone, D., Dunmore, R., Hamilton, J., Hopkins, J. R., Lee, J. D., Lewis, A.C., Williams, P., Kleffmann, J., Laufs, S., Woodward-Massey, R., Heard, D. E.: Understanding in situ ozone production in the summertime through radical observations and modelling studies during the Clean air for London project (ClearfLo), Atmos. Chem. Phys., 18, 2547-2571, https://doi.org/10.5194/acp-18-2547-2018, 2018.

Woodward-Massey, R., Observations of radicals in the atmosphere: measurement validation and model comparisons, PhD Thesis, http://etheses.whiterose.ac.uk/22164/, 2018.

Xu, L., Kollman, M. S., Song, C., Shiling, J. E., and Ng, N. L.: Effects of NOx on the volatility of secondary organic aerosol from isoprene photooxidation, Environ. Sci. Technol., 48, 2253-2262, https://doi.org/10.1021/es404842g, 2014.

Zhang, H., Lin, Y, -H., Zhang, Z., Zhang, X., Shaw, S. L., Knipping, E. M., Weber, R. J., Gold, A., Kamens, R. M., and Surratt, J. D.: Secondary organic aerosol formation from methacrolein photooxidation: Roles of NO_X level, relative humidity and aerosol acidity, Environ. Chem., 9, 247-262, https://doi.org/10.1071/EN12004, 2012.

Zhang, H., Surratt, J. D., Lin, Y. H., Bapat, J., and Kamens, R.M.: Effect of relative humidity on SOA formation from isoprene/NO photooxidation: Enhancement of 2-methylglyceric acid and its corresponding oligoesters under dry conditions, Atmos. Chem. Phys., 11, 6411-6424, https://doi.org/10.5194/acp-11-6411-2011, 2011.

Zhang, Q., Jimenez, J. L., Canagaratna, M. R., Ulbrich, I. M., Ng, N. L., Worsnop, D. R., and Sun, Y.: Understanding atmospheric organic aerosols via factor analysis of aerosol mass spectrometry: a review, Anal. Bioanal. Chem., 401, 3045-3067, https://doi.org/10.1007/s00216-011-5355-y, 2011.

Zhang, Y., Chen, Y., Lambe, A. T., Olson, N. E., Lei, Z., Craig, R. L., Zhang, Z., Gold, A., Onasch, T. B., Jayne, J. T., Worsnop, D. R., Gaston, C. J., Thornton, J. A., Vizuete, W., Ault, A. P., and Surratt, J. D.: Effect of the Aerosol-Phase State on Secondary Organic Aerosol Formation from the Reactive Uptake of Isoprene-Derived Epoxydiols (IEPOX), Environ. Sci. Technol. Lett., 5, 167-174, https://doi.org/10.1021/acs.estlett.8b00044, 2018.

Zhang, Y., Ren, H., Sun, Y., Cao, F., Chang, Y., Liu, Shoudong, L., Lee, X., Agrios, K., Kawamura, K., Liu, D., Ren, L., Du, W., Wang, Z., Prévôt, A. S. H., Szidat, S., and Fu, P.: High Contribution of Nonfossil Sources to Submicrometer Organic Aerosols in Beijing, China, Environ. Sci. Technol., 51, 7842-7852, ~~https://doi.org/10.1021/acs.est.7b01517,~~ https://doi.org/10.1021/acs.est.7b01517, 2017.

Zhang, Y., Sun, J., Zhang, X., Shen, X., Wang, T., and Qin, M.: Seasonal characterization of components and size distributions for submicron aerosols in Beijing, Sci. China Earth Sci., 56, 890-900, https://doi.org/10.1007/s11430-012-4515-z, 2013.

Zhang, Y., Tang, L., Sun, Y., Favez, O., Canonaco, F., Albinet, A., Couvidat, F., Liu, D., Jayne, J. T., Wang, Z., Croteau, P. L., Canagaratna, M. R., Zhou, H., Prévôt, A. S. H., and Worsnop, D. R.: Limited formation of isoprene epoxydiols-derived secondary organic aerosol under NO_X-rich environments in Eastern China, Geophys. Res. Lett., 44, 2035-2043, https://doi.org/10.1002/2016GL072368, 2017.

Zhou, W., Zhao, J., Ouyang, B., Mehra, A., Xu, W., Wang, Y., Bannan, T. J., Worrall, S. D., Priestley, M., Bacak, A., Chen, Q., Xie, C., Wang, Q., Wang, J., Du, W., Zhang, Y., Ge, X., Ye, P., Lee, J. D., Fu, P., Wang, Z., Worsnop, D., Jones, R., Percival, C. J., Coe, H., and Sun, Y.: Production of N_2O_5 and $ClNO_2$ in summer in urban Beijing, China, Atmos. Chem. Phys., 18, 11581-11597, https://doi.org/10.5194/acp-18-11581-2018, 2018.

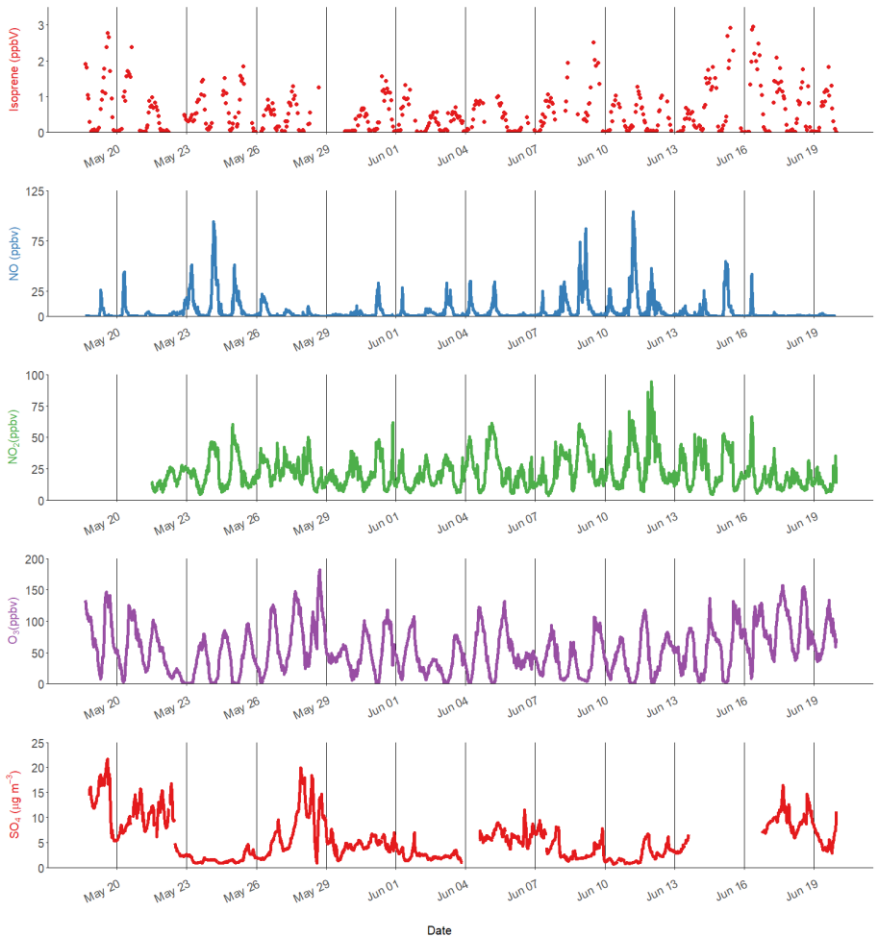

Figure 1. Time series of isoprene, nitric oxide (NO), nitrogen dioxide (NO_2), ozone (O_3) and particulate sulfate (SO_4). The black lines are at midnight every 72 hours.

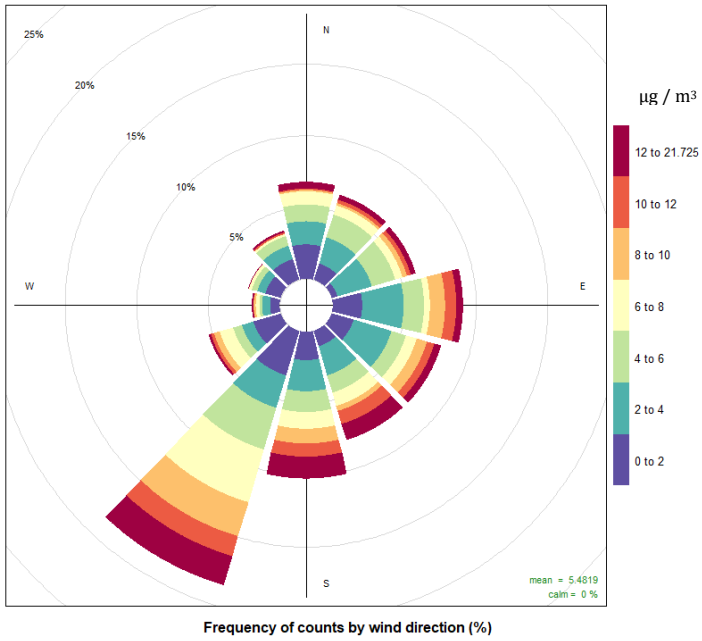

Figure 2. PollutionRose plot (Openair) of particulate sulfate measured by AMS, for the sampling period.

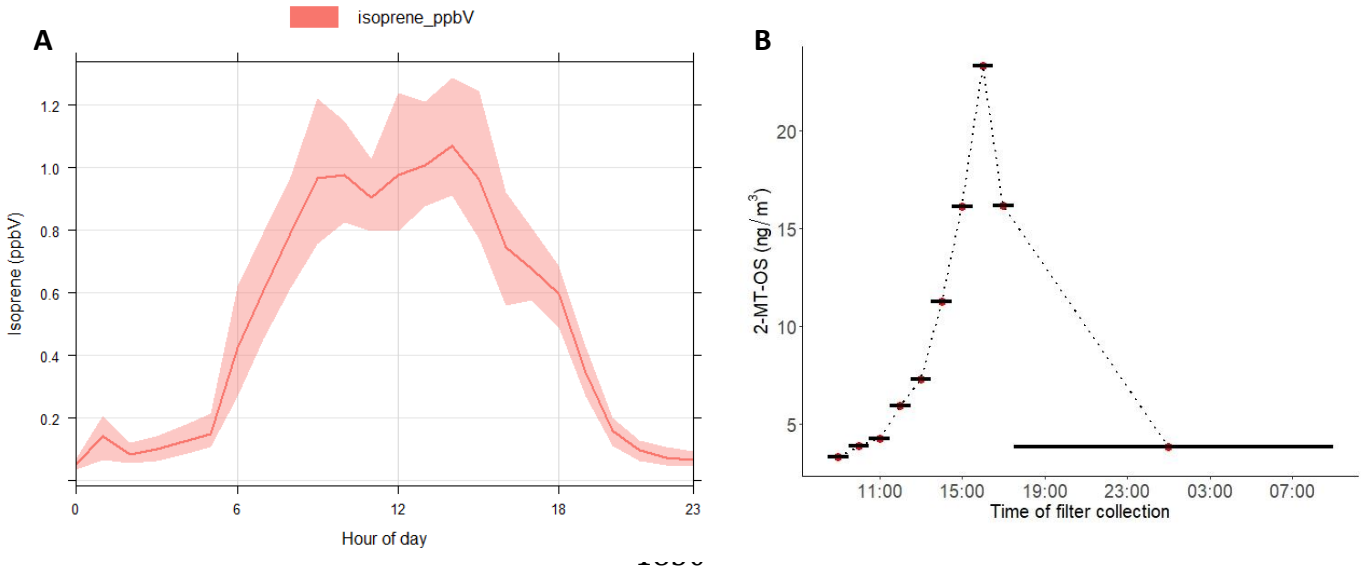

Figure 3. (A) Average diurnal profile of isoprene mixing ratio measured using DC-GC-FID. (B) Diurnal profile of 2-methyltetrol sulfate (2-MT-OS) in particulate matter ($PM_{2.5}$) collected on filters hourly over the 11th to 12th June 2017. Black lines indicate length of filter sampling period.

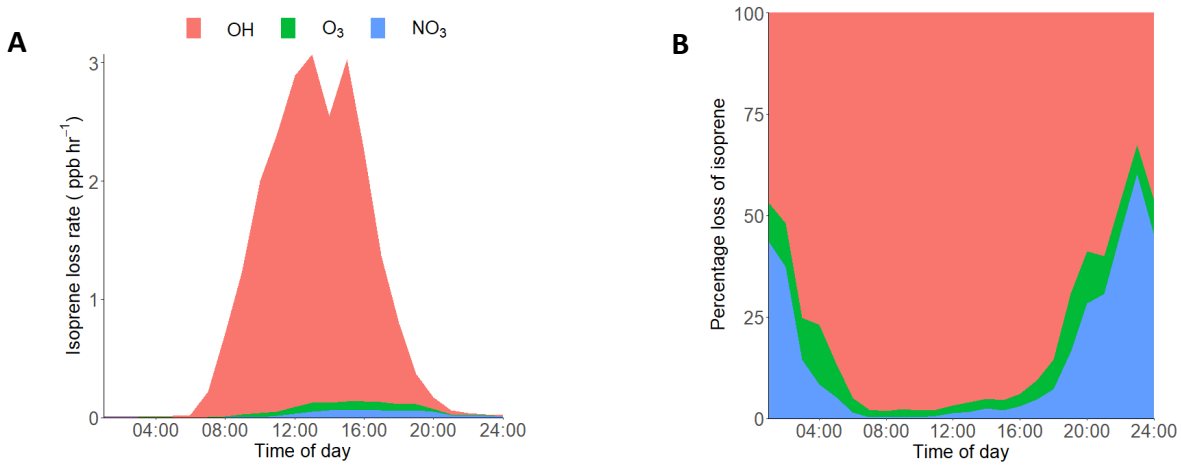

Figure 4. (A) Diurnal loss rate of isoprene calculated using measured average diurnal profiles of isoprene, OH, NO_3 and ozone. (B) Average diurnal of the percentage loss of isoprene from reactions with OH, O_3 and NO_3 radicals.The IUPAC rate constants used for the calculations are as follows, NO_3: $7x10^{-13}$, O_3:$1.27x10^{17}$, OH: $1x10^{10}$ cm^3 $molecule^{-1}$ s^{-1} (Atkinson et al., 2006).

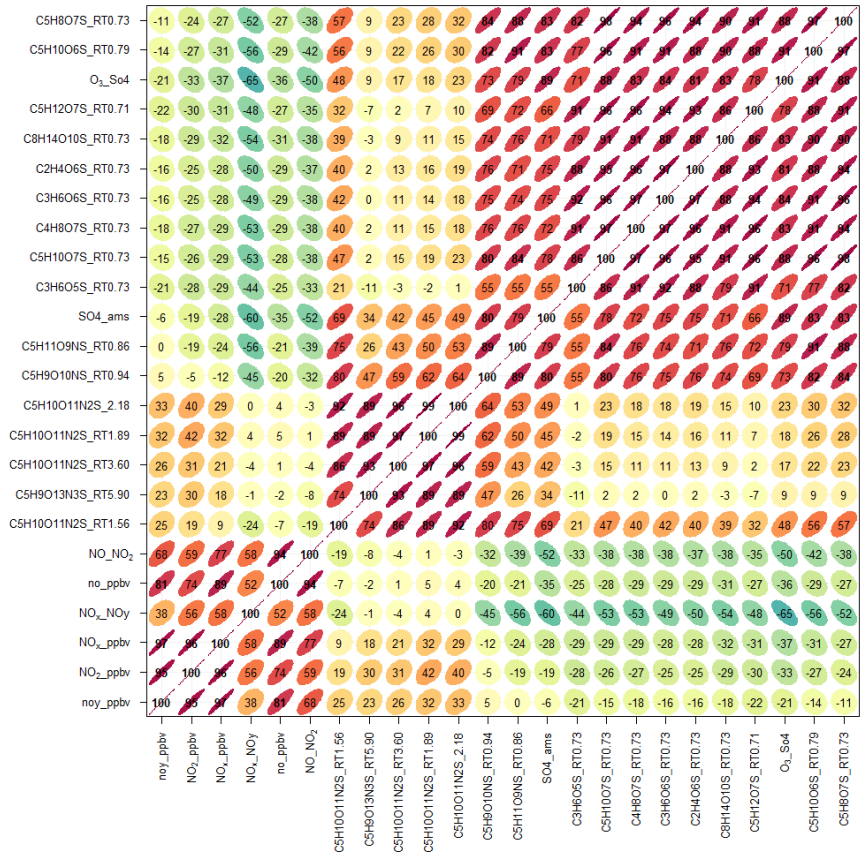

Figure 5. Corplot (Openair) highlighting the correlations between known iSOA tracers and anthropogenic pollutants. The number represents the R correlation between the two species. With redder more elongated circles highlighting a higher correlation.

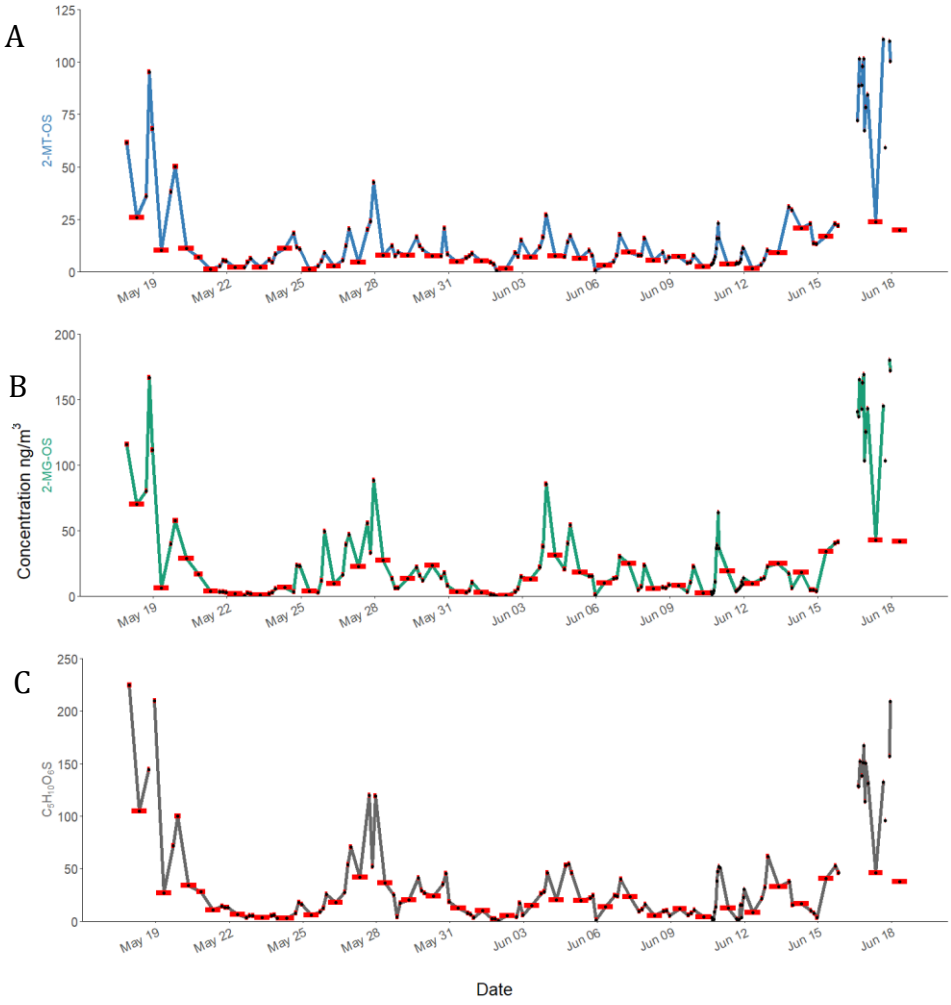

Figure 6. Time series of observed concentrations of iSOA tracers in Beijing during APHH. (A) 2-MT-OS ($C_5H_{12}O_7S$) (B) 2-MG-OS ($C_4H_8O_7S$) (C) $C_5H_{10}SO_6$. The red bars indicate the length of the sampling time. The individual sample times will be given in the accompanying dataset. *(doi to be given on acceptance)*

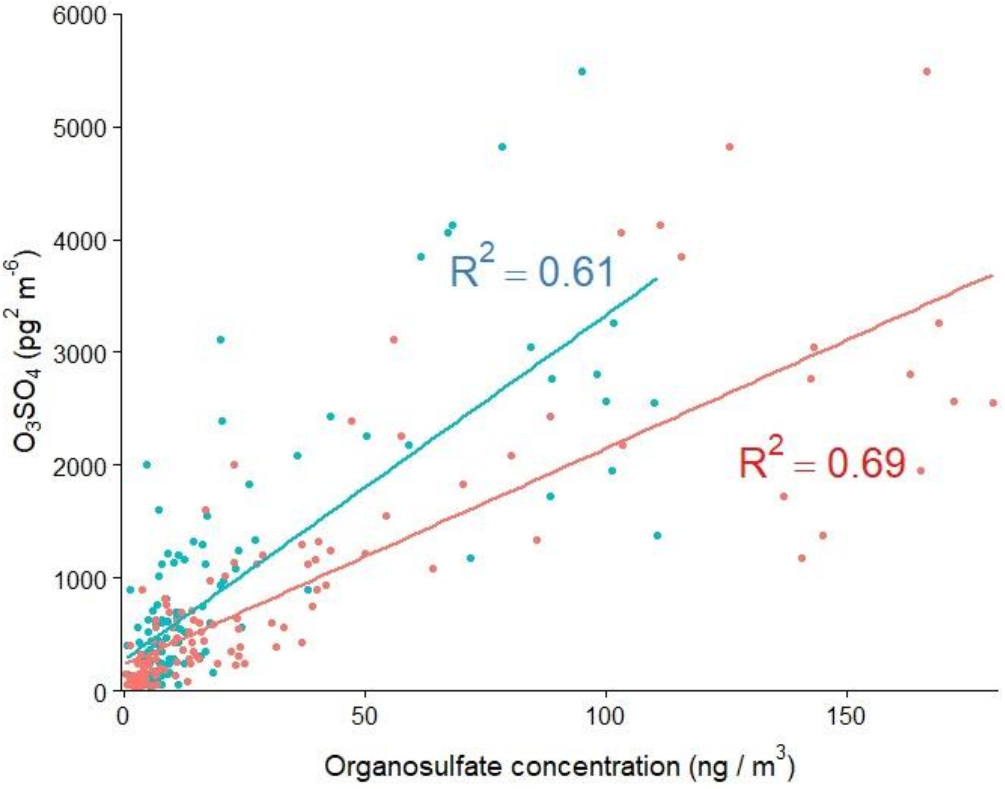

Figure 7. Plot of 2-MT-OS ($C_5H_{12}O_7S$, blue) and 2-MG-OS ($C_4H_8O_7S$, red) concentrations versus [Ozone][SO_4]. The high time resolution data (O_3 and AMS SO_4^{2-}) has been averaged to the filter sampling time. The line was calculated using the stat_smooth function in the R package ggplot2, using the method "lm".

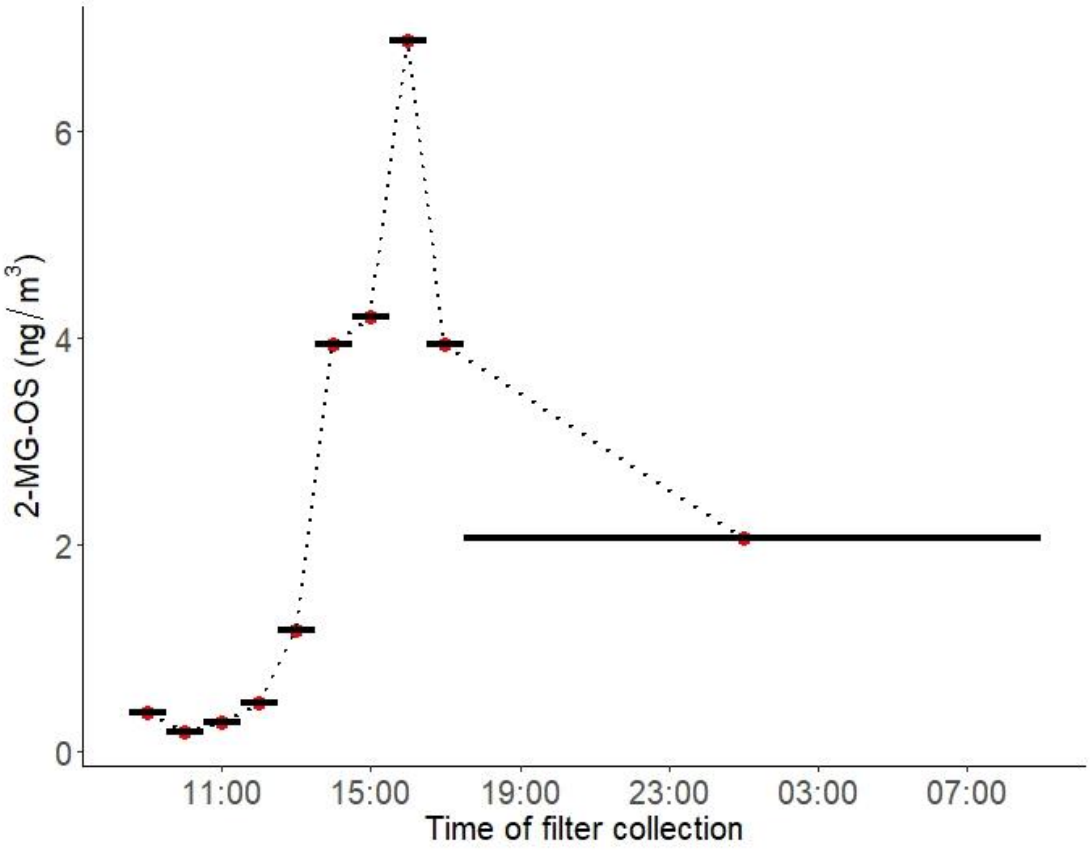

Figure 8. Diurnal profile of 2-methylglyceric acid sulphate (2-MG-OS) in particulate matter collected on filters hourly over the 11th to 12th June 2017. Black lines indicate length of sampling.

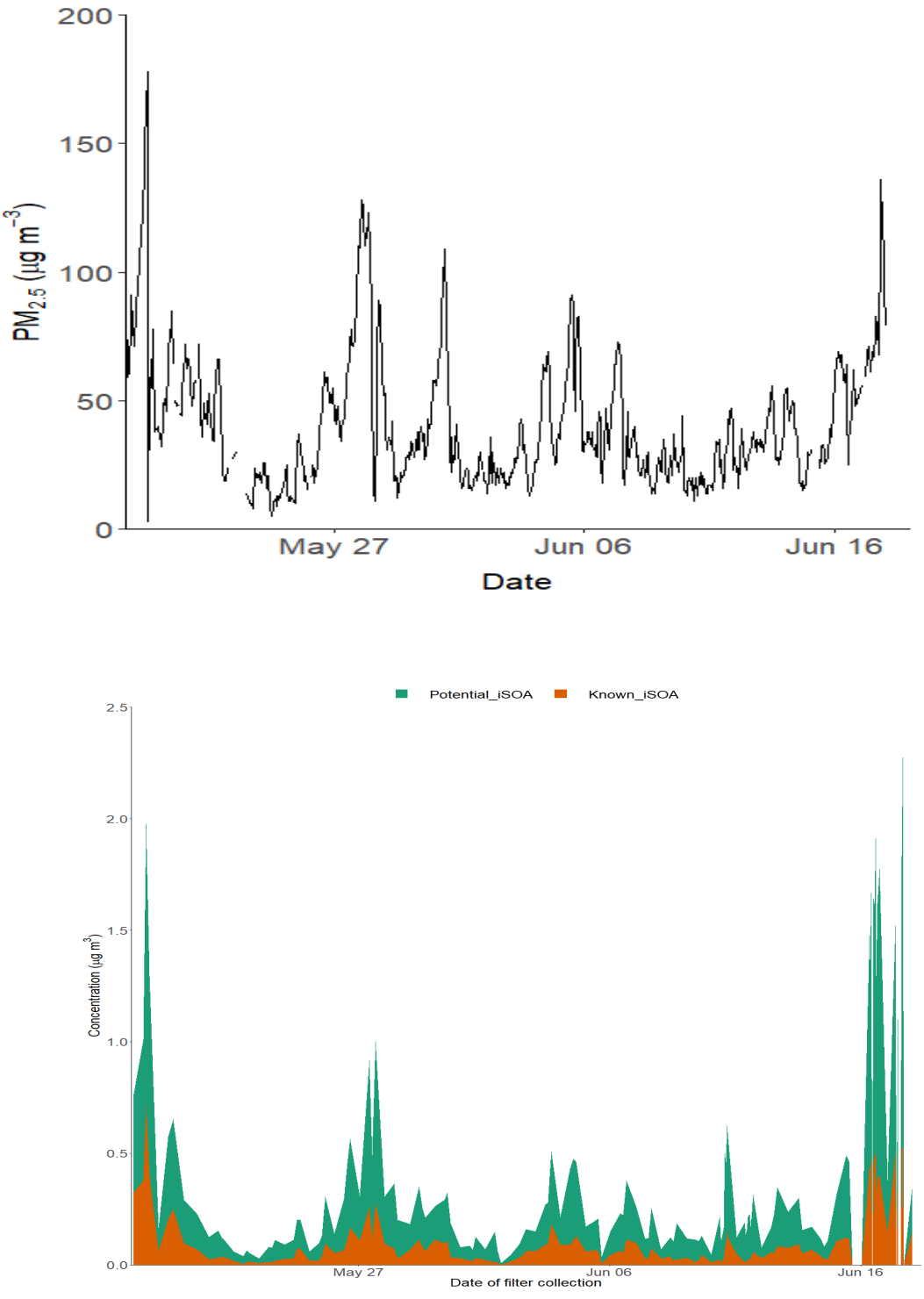

Figure 9. A) Time series of $PM_{2.5}$ over the sampling period. B) Time series of the total known isoprene SOA signal (2-MT-OS, 2-MG-OS, $C_5H_{10}SO_7$ (MW 214) $C_5H_8SO_7$ (MW 212) $C_5H_{11}NSO_9$ (MW 261), $C_5H_9NSO_{10}$ (MW 275) $C_5H_{10}O_{11}N_2S$ (MW 306), $C_5H_9O_{13}N_3S$ (MW 351) and the total signal from the other iSOA tracers quantified in this study.

Table 1. Supplementary anthropogenic pollutants measured during the sampling period analysed in this study.

Pollutant	Mean ± SD	Max	Min
O_3 (ppbv)	54.0 ± 37.5	181.8	2.0
NO (ppbv)	5.1 ± 11.3	104.1	0.1
NO_2 (ppbv)	22.3 ± 13.0	94.5	3.7
SO_4 (µg/m^{-3})	5.5 ± 4.1	21.7	0.7

Table 2. Molecular formulas, negative ion masses, retention times (RT), time weighted means (ng m^{-3}) for the entire sampling period and original reference to where the tracer was found of each proposed iSOA tracer. BD = Below detection. The estimated uncertainties were discussed in section 3.4 as 60 %, accounting for the use of the matrix correction factors.

Isoprene Tracer	$[M-H]^{-1}$	RT (min)	Time weighted mean (ng m^{-3})	Maximum (ng m^{-3})	Minimum (ng m^{-3})	Reference
$C_2H_4O_6S$	154.9656	0.73	38.4	366.1	BD	Surratt et al., 2008
$C_5H_{10}O_6S$	197.0125	0.79	28.7	336.2	0.25	Surratt et al., 2007
$C_5H_{10}O_5S$	181.0176	0.93	26.5	448.5	2.91	Nguyen et al., 2010
$C_4H_8O_6S$	182.9969	0.73	21.7	229.1	0.50	Riva et al., 2016
$C_4H_8O_7S$	198.9918	0.73	21.5	180.5	0.32	Surratt et al., 2007
$C_3H_6O_5S$	152.9863	0.73	20.5	327.9	0.98	Surratt et al., 2008
$C_3H_6O_6S$	168.9812	0.73	14.5	137.7	0.25	Surratt et al., 2008
$C_5H_8O_7S$	210.9918	0.73	14.0	136.4	0.27	Surratt et al., 2008
$C_5H_{11}O_9NS$	260.0082	0.86	12.6	154.1	0.10	Surratt et al., 2008
$C_5H_{12}O_7S$	215.0231	0.71	11.8	110.9	0.77	Surratt et al., 2008
$C_5H_{10}O_7S$	213.0075	0.73	10.6	104.7	0.38	Surratt et al., 2008
$C_5H_9O_{10}NS$	273.9874	0.94	9.17	53.8	BD	Nestorowicz et al., 2018
$C_4H_8O_5S$	167.0019	0.73	9.10	114.5	0.68	Surratt et al., 2007
$C_5H_8O_5S$	179.0020	0.85	6.59	144.2	0.43	Riva et al., 2016
$C_5H_{10}O_5S$	181.0176	1.24	4.90	36.3	1.21	Riva et al., 2016
$C_5H_{10}O_8S$	229.0024	0.75	4.59	40.9	BD	Nestorowicz et al., 2018
$C_5H_8O_9S$	242.9816	0.64	1.55	13.9	BD	Nestorowicz et al., 2018
$C_5H_{10}O_{11}N_2S$	304.9783	2.18	1.04	8.62	BD	Surratt et al., 2008
$C_{10}H_{20}O_8S$	299.0806	1.65	1.01	8.38	BD	Riva et al., 2016
$C_5H_{10}O_{11}N_2S$	304.9783	1.89	0.83	7.69	BD	Surratt et al., 2008
$C_8H_{14}O_{10}S$	301.0235	0.73	0.57	4.16	BD	Surratt et al., 2007
$C_5H_{10}O_{11}N_2S$	304.9783	1.56	0.42	2.90	BD	Surratt et al., 2008
$C_{10}H_{18}O_7S$	281.0701	1.03	0.33	6.76	BD	Riva et al., 2016
$C_5H_{10}O_{11}N_2S$	304.9783	3.60	0.31	3.32	BD	Surratt et al., 2008
$C_5H_9O_{13}N_3S$	349.9783	5.90	0.19	2.04	BD	Ng et al., 2008
$C_{10}H_{18}O_8S$	297.0650	0.75	0.14	5.25	BD	Riva et al., 2016
$C_5H_{11}O_8NS$	244.0133	1.93	0.11	1.46	BD	Nestorowicz et al., 2018
$C_5H_9O_{13}N_3S$	349.9783	5.49	0.02	0.17	BD	Ng et al., 2008
$C_5H_9O_{13}N_3S$	349.9783	5.34	0.008	0.10	BD	Ng et al., 2008
$C_5H_{12}O_8S$	231.0180	0.75	0.005	0.50	BD	Riva et al., 2016
$C_{10}H_{20}O_9S$	315.0755	1.46	0.002	0.21	BD	Riva et al., 2016

Table 3. Isoprene CHO tracer concentrations measured via GC-MS using 24-hour samples between 22/05/2017 and 22/06/2017. 2-MTs is equal to the sum of 2-methylthreitol and 2-methylerythritol and the C5-alkene triols is equal to the sum of cis-2-methyl-1,3,4-trihydroxy-1-butene, 3-methyl-2,3,4-trihydroxy-1-butene and trans-2-methyl-1,3,4-trihydroxy-1-butene.

Isoprene Tracer	Min (ng m^{-3})	Max (ng m^{-3})	Average (ng m^{-3})
2-MTs	4.55	52.67	17.29
MG	1.38	15.53	7.24
C_5-alkene triols	0.23	1.08	0.51

Table 34. Comparison of concentrations of iSOA tracer concentrations and ratios in previous studies in the Amazon, SE USA and China. *Selected sample not an average concentration.

Location															
				Mean Concentration (ng m^{-3})						**Ratio low to high NO**		**Ratio CHO:CHOS**		
				2-MT	**2-MT-OS**	**2-MG**	**2-MG-OS**			**2-MT:2-MG**	**2-MT-OS:2-MG-OS**	**2-MT:2-MT-OS**	**2-MG:2-MG-OS**	**Reference**
China Urban, Beijing (2017)	China Rural, NCP (2013)	China Regional, Beijing (2016)	China Regional, PRD (2008)	SE US, Atlanta (2015)	SE US, Look Rock (2013)	SE US, Look Rock (2013)	SE US, Centreville (2013)	Amazon, T3 (2014)	Amazon, Manuas (2016)						
17.3	44		91.5		861*	163.1			137*						
11.8		5.3	2.2	1792	2334*	169.5	217	83(wet)/ 399(dry)	390*						
7.2	19.3		7.7			7.5									
21.5		3.6	1.4	53		10	10.7	0.7(wet)/ 30(dry)							
2.40	2.30		11.9			21.7									
0.55		1.47	1.57	33.8		17.0	20.3	118(wet) / 13(dry)							
1.47			41.6		0.37	0.96			0.35						
0.33			5.51			0.75									
This work	Li et al., 2018	Wang et al., 2018	He et al., 2018	Hettiyadura et al., 2019	Cui et al., 2018	Budlisulistiorini et al.,	Riva et al., 2019	Glasius et al., 2018	Cui et al., 2018						